(26) Lee, H. J.; Lee, E. Y.; Kwon, M. S.; Paik, Y. K. Biomarker discovery from the plasma proteome using multidimensional fractionation proteomics. *Curr. Opin. Chem. Biol.* **2006**, *10* (1), 42–49.

(27) Dea, M. K.; Hamilton-Wessler, M.; Ader, M.; Moore, D.; Schaffer, L.; Loftager, M.; Volund, A.; Bergman, R. N. Albumin binding of acylated insulin (NN304) does not deter action to stimulate glucose uptake. *Diabetes* **2002**, *51* (3), 762–769.

(28) Curry, S. Beyond expansion: structural studies on the transport roles of human serum albumin. *Vox Sang.* **2002**, *83* (Suppl. 1), 315–319.

(29) Schussler, G. C. The thyroxine-binding proteins. *Thyroid* **2000**, *10* (2), 141–149.

(30) Chertov, O.; Biragyn, A.; Kwak, L. W.; Simpson, J. T.; Boronina, T.; Hoang, V. M.; Prieto, D. A.; Conrads, T. P.; Veenstra, T. D.; Fisher, R. J. Organic solvent extraction of proteins and peptides from serum as an effective sample preparation for detection and identification of biomarkers by mass spectrometry. *Proteomics* **2004**, *4* (4), 1195–1203.

(31) Merrell, K.; Southwick, K.; Graves, S. W.; Esplin, M. S.; Lewis, N. E.; Thulin, C. D. Analysis of low-abundance, low-molecular-weight serum proteins using mass spectrometry. *J. Biomol. Tech.* **2004**, *15* (4), 238–248.

(32) Zheng, X.; Baker, H.; Hancock, W. S. Analysis of the low molecular weight plasma peptidome using ultrafiltration and a hybrid ion trap-Fourier transform mass spectrometer. *J. Chromatogr., A* **2006**, *1120* (1–2), 173–184.

(33) Terracciano, R.; Gaspari, M.; Testa, F.; Pasqua, L.; Tagliaferri, P.; Cheng, M. M.; Nijdam, A. J.; Petricoin, E. F.; Liotta, L. A.; Cuda, G.; Ferrari, M.; Venuta, S. Selective binding and enrichment for low-molecular weight biomarker molecules in human plasma after exposure to nanoporous silica particles. *Proteomics* **2006**, *6* (11), 3243–3250.

(34) Shen, W.; Xiong, H.; Xu, Y.; Cai, S.; Lu, H.; Yang, P. ZnO-poly(methyl methacrylate) nanobeads for enriching and desalting low-abundant proteins followed by directly MALDI-TOF MS analysis. *Anal. Chem.* **2008**, *80* (17), 6758–6763.

(35) Righetti, P. G.; Boschetti, E.; Lomas, L.; Citterio, A. Protein Equalizer Technology: the quest for a democratic proteome. *Proteomics* **2006**, *6* (14), 3980–3992.

(36) Tammen, H.; Schulte, I.; Hess, R.; Menzel, C.; Kellmann, M.; Mohring, T.; Schulz-Knappe, P. Peptidomic analysis of human blood specimens: comparison between plasma specimens and serum by differential peptide display. *Proteomics* **2005**, *5* (13), 3414–3422.

(37) Tammen, H.; Mohring, T.; Kellmann, M.; Pich, A.; Kreipe, H. H.; Hess, R. Mass spectrometric phenotyping of Val34Leu polymorphism of blood coagulation factor XIII by differential peptide display. *Clin. Chem.* **2004**, *50* (3), 545–551.

(38) Li, Y.; Bai, Q.; Chen, G.; Wang, L. Fast separation and preparation of proteomics samples of human serum using high performance hydrophobic interaction chromatographic cake. *Sepu* **2008**, *26* (3), 331–334.

(39) Harper, R. G.; Workman, S. R.; Schuetzner, S.; Timperman, A. T.; Sutton, J. N. Low-molecular-weight human serum proteome using ultrafiltration, isoelectric focusing, and mass spectrometry. *Electrophoresis* **2004**, *25* (9), 1299–1306.

(40) Lopez, M. F.; Mikulskis, A.; Kuzdzal, S.; Golenko, E.; Petricoin, E. F., 3rd; Liotta, L. A.; Patton, W. F.; Whiteley, G. R.; Rosenblatt, K.; Gurnani, P.; Nandi, A.; Neill, S.; Cullen, S.; O'Gorman, M.; Sarracino, D.; Lynch, C.; Johnson, A.; Mckenzie, W.; Fishman, D. A novel, high-throughput workflow for discovery and identification of serum carrier protein-bound peptide biomarker candidates in ovarian cancer samples. *Clin. Chem.* **2007**, *53* (6), 1067–1074.

(41) Lopez, M. F.; Mikulskis, A.; Kuzdzal, S.; Bennett, D. A.; Kelly, J.; Golenko, E.; DiCesare, J.; Denoyer, E.; Patton, W. F.; Ediger, R.; Sapp, L.; Ziegert, T.; Lynch, C.; Kramer, S.; Whiteley, G. R.; Wall, M. R.; Mannion, D. P.; Della Cioppa, G.; Rakitan, J. S.; Wolfe, G. M. High-resolution serum proteomic profiling of Alzheimer disease samples reveals disease-specific, carrier-protein-bound mass signatures. *Clin. Chem.* **2005**, *51* (10), 1946–1954.

(42) Schagger, H.; von Jagow, G. Tricine-sodium dodecyl sulfate-polyacrylamide gel electrophoresis for the separation of proteins in the range from 1 to 100 kDa. *Anal. Biochem.* **1987**, *166* (2), 368–379.

(43) Fukutomi, T.; Kodera, Y.; Kogo, T.; Furudate, S.; Omori, A.; Maeda, T. A simple method for peptide purification as a basis for peptidome analysis. *J. Electrophoresis* **2005**, *49* (1), 15–21.

(44) Takahashi, A.; Yasuda, A.; Sullivan, C. V.; Kawauchi, H. Identification of proopiomelanocortin-related peptides in the rostral pars distalis of the pituitary in coelacanth: evolutional implications. *Gen. Comp. Endocrinol.* **2003**, *130* (3), 340–349.

(45) Takahashi, A.; Takasaka, T.; Yasuda, A.; Amemiya, Y.; Sakai, M.; Kawauchi, H. Identification of carp proopiomelanocortin-related peptides and their effects on phagocytes. *Fish Shellfish Immunol.* **2000**, *10* (3), 273–284.

(46) Cheng, A. J.; Chen, L. C.; Chien, K. Y.; Chen, Y. J.; Chang, J. T.; Wang, H. M.; Liao, C. T.; Chen, I. H. Oral cancer plasma tumor marker identified with bead-based affinity-fractionated proteomic technology. *Clin. Chem.* **2005**, *51* (12), 2236–2244.

(47) Sy, S. M.; Lai, P. B.; Pang, E.; Wong, N. L.; To, K. F.; Johnson, P. J.; Wong, N. Novel identification of zyxin upregulations in the motile phenotype of hepatocellular carcinoma. *Mod. Pathol.* **2006**, *19* (8), 1108–1116.

(48) Watanabe, M.; Takemasa, I.; Kawaguchi, N.; Miyake, M.; Nishimura, N.; Matsubara, T.; Matsuo, E.; Sekimoto, M.; Nagai, K.; Matsuura, N.; Monden, M.; Nishimura, O. An application of the 2-nitrobenzenesulfenyl method to proteomic profiling of human colorectal carcinoma: A novel approach for biomarker discovery. *Proteomics: Clin. Appl.* **2008**, *2* (6), 925–935.

(49) Jacobs, J. M.; Adkins, J. N.; Qian, W. J.; Liu, T.; Shen, Y.; Camp, D. G., 2nd; Smith, R. D. Utilizing human blood plasma for proteomic biomarker discovery. *J. Proteome Res.* **2005**, *4* (4), 1073–1085.

PR9008018
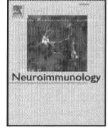
Serum levels of complement C4 fragments correlate with disease activity in multiple sclerosis: Proteomic analysis

Setsu Sawai [a,*], Hiroshi Umemura [a], Masahiro Mori [b], Mamoru Satoh [a], Sei Hayakawa [b], Yoshio Kodera [c], Takeshi Tomonaga [a], Satoshi Kuwabara [b], Fumio Nomura [a]

[a] Department of Molecular Diagnosis, Graduate School of Medicine, Chiba University, 1-8-1 Inohana, Chuo-ku, Chiba 260-8670, Japan
[b] Department of Neurology, Graduate School of Medicine, Chiba University, Chiba, Japan
[c] Department of Physics, School of Science, Kitasato University, Kanagawa, Japan

A R T I C L E   I N F O

A B S T R A C T

To detect serum biomarkers associated with disease activity in relapsing–remitting multiple sclerosis (MS). We studied serum low-molecular peptide profiling of MS patients and normal controls comprehensively by matrix-assisted laser desorption/ionization time-of-flight mass spectrometry. Serum level of 1741 Da peptide was increased at the time of clinical relapse in patients than in normal controls and returned toward normal during remission. Tandem mass spectrometry analysis revealed that the peptide was a fragment of complement C4 (NGFKSHALQLNNRQI). This fragment peptide could be a possible marker of disease activity. It may reflect complement activation in the pathogenesis of MS.

© 2009 Elsevier B.V. All rights reserved.

1. Introduction

Multiple sclerosis (MS) is an autoimmune inflammatory demyelinating disease of the central nervous system. In most MS patients, this disorder is characterized by a relapsing–remitting course (Polman et al., 2005). The clinical course of MS varies greatly among individuals, which is possibly triggered by a complex interplay of multiple genetic (International Multiple Sclerosis Genetics Consortium, 2007), infectious (Steiner et al., 2001), and environmental factors (Koning et al., 2007).

The importance of early treatment at the time of MS relapse has been emphasized (Frohman et al., 2006; Pittock et al., 2006). Moreover, new therapeutic agents such as natalizumab (Polman et al., 2006; Rudick et al., 2006; Kappos et al., 2007), fingolimod (Kappos et al., 2006), and alemtuzumab (Coles et al., 1999) have been used in MS patients to prevent relapse. It is clinically useful to find biomarkers that correlate with disease activity in MS, because this would enable the prediction of relapses and the early initiation of therapeutic interventions. Many studies have investigated serum or cerebrospinal fluid (CSF) biomarkers such as cytokines (Onodera et al., 1999), chemokines and their receptors (Mahad et al., 2003), matrix metalloproteinases (Kanesaka et al., 2006), cell surface antigen (Frisullo et al., 2006; Aranami et al., 2006), and adhesion molecules (Kuenz et al., 2005) in relation to episodes of MS

relapse. However, these biomarkers are not used clinically because their measurement is time consuming and the sensitivity of the measurement methods is insufficient. Therefore, more reliable methods need to be developed. Proteomic analysis is a novel method for detecting peptide biomarkers in a variety of disorders.

A recent study using proteomic analysis detected a cleavage product of the protein cystatin C in the CSF of MS patients; this cleavage product is a potential biomarker for a subgroup of MS patients (Irani et al., 2006). However, a later report suggests that this cleavage product is merely a freezing artifact caused by freeze–thaw cycles (Del Boccio et al., 2007). Many previous studies have investigated biomarkers in CSF, but biomarkers in serum are more convenient for monitoring disease activity in clinical practice.

We therefore performed proteomic analyses to evaluate the serum profiles of low-molecular-weight peptides by matrix-assisted laser desorption/ionization time-of-flight (MALDI-TOF) mass spectrometry in patients with MS.

2. Materials and methods

2.1. Patients and blood sample preparation

Sera were collected from 31 patients with relapsing–remitting MS (10 men; median age: 34 years; range: 21–78 years) at the time of clinical relapse. Of the 31 patients, 18 relapses occurred in the spinal cord, 4 in the cerebral hemisphere, 8 in the brainstem, and 1 in the optic nerve. In the four patients with brain lesion, relapse was confirmed by gadolinium-enhancing MRI. At the time of relapse, 8 patients out of 31

patients in this study received interferon-beta therapy. After relapse, 21 patients received steroid pulse therapy, and 9 were treated with oral prednisolone.

Sera from 47 healthy subjects (10 men; median age: 38 years; range: 21–62 years) served as normal controls. As disease controls, sera were collected from 11 patients with Guillain–Barré syndrome within 2 weeks after the neurological onset. All MS patients fulfilled the diagnostic criteria (Polman et al., 2005). Sera were also obtained from 16 MS patients during remission 3–6 months after the relapse. After the blood samples were collected, they were allowed to clot at room temperature for about 2 h and were then centrifuged at 3000×g for 5 min. Sera were stored in aliquots at −80 °C. All subjects gave informed consent to the procedures, which were approved by the Ethics Committee of Chiba University School of Medicine.

2.2. Chemicals and calibrators

2-Cyano-4-hydroxycinnamic acid (CHCA) matrix solution (Bruker Daltonics, Bremen, Germany) was diluted to 0.3 g/l in an ethanol: acetone (2:1) solution. Acetone and ethanol were of HPLC-grade and were purchased from Wako Pure Chemical Industries (Osaka, Japan). The calibrator used was the Peptide Calibration Standard II (Bruker Daltonics).

2.3. Serum pretreatment with WCX magnetic beads by ClinProtRobot

Serum samples (5 µl) were prefractionated using Magnetic-Beads-based Weak Cation Exchange Chromatography resins (MB-WCX) (Bruker Daltonics) by ClinProtRobot automatic machine. A 5-µl serum sample was mixed with 10 µl binding solution; 5 µl MB-WCX was then added, and the solution was mixed. Next, the tube was placed in a magnetic bead separator to allow separation of the unbound solution, and the supernatant was removed. The beads were then washed three times with 100 µl wash buffer, after which the proteins and peptides were eluted from the magnetic beads with 10 µl of an elution solution and 10 µl of a stabilization solution. The eluate was diluted 1:10 in a CHCA matrix solution. Next, 1 µl of the mixture was spotted onto an AnchorChip target (Bruker Daltonics) and then left to dry for several minutes at room temperature. All procedures were performed according to the protocols described elsewhere (Umemura et al., 2009; Zhang et al., 2004; Ebert et al., 2006).

2.4. Mass spectrometry

The AnchorChip target plate was placed in an AutoFlex® II TOF/TOF mass spectrometer (Bruker Daltonics) controlled by Flexcontrol 2.4 software (Bruker Daltonics). This instrument is equipped with a 337-nm nitrogen laser, delayed-extraction electronics, and a 25-Hz digitizer. All acquisitions were generated by an automated acquisition method included in the instrument software and based on averaging 1000 randomized shots. Spectra were acquired in the positive linear mode in a molecular mass range from 600 to 10,000 Da. Peak clusters were completed using the second-pass peak section (signal-to-noise ratio > 5). The relative peak intensities, normalized to a total ion current of m/z between 600 and 10,000, were expressed as arbitrary units. All spectra ranging from 1000 to 4000 m/z obtained by MALDI-TOF mass spectrometry were analyzed using Bruker Daltonics flexAnalysis 2.1 software and ClinProTools 2.1 software.

2.5. Peptide identification

The MALDI-tandem mass spectrometry spectrum was recorded using an AutoFlex® II TOF/TOF mass spectrometer (Bruker Daltonics) in the LIFT mode. Six hundred laser shots from the parent 2500 laser shots for the fragments were summed up. The MALDI-tandem mass spectrometry spectrum was subjected to a database search using the

Mascot (Matrixscience, UK) database search engine. The search parameters were as follows: no enzyme specificity, 25 ppm mass tolerance for the parent mass, and 1 Da for the fragment masses. No fixed modification or oxidation (M) for variable modifications was selected. The IPI human database (July 2, 2008) was searched.

3. Results

3.1. MALDI-TOF MS analysis of peptides in sera from MS patients

Peak intensities of 10 peptides were significantly different in the MS and healthy control groups; 7 of these peptides were increased and the remaining 3 peptides were decreased in the MS sera. Next, we compared the peptide profiling in the relapsing and remitting phases in MS by using MALDI-TOF mass spectrometry. Of the 10 peptide peaks, which were different between the MS and healthy controls, the intensity of only one peptide peak with an m/z value of 1741 Da was significantly changed in the relapsing and remitting phases. The serum level of the peptide increased at the time of relapse and decreased during remission.

As shown in Fig. 1, the mean serum level of the 1741-Da peptide was significantly greater ($p = 0.0001$) in MS patients (46.0 arbitrary units) than in healthy controls (28.8 arbitrary units), but in patients with Guillain–Barré syndrome it was not increased (32.8 arbitrary units) compared with healthy controls ($p = 0.28$). Serum levels of the 1741-Da peptide were compared in relapsing MS patients treated and those not treated with interferon-beta (Supplementary Fig. A2), but there was no significant difference in the peptide levels between the two patient groups. Serial analysis showed that in 13 of the 16 patients, the 1741-Da peptide was increased in the relapsing phase and was decreased during remission ($p = 0.01$; Fig. 2).

3.2. Identification of a fragment of complement C4 by proteome analysis

The exact mass of the peak was determined by MALDI-TOF in the reflectron mode. The spectrum was recorded directly from one of the preparations used for the profiling experiment. Subsequently, a MALDI-tandem mass spectrometry spectrum was recorded using that signal. This spectrum was submitted to a database search. The Mascot search engine reported that the peptide was a partial sequence of complement C4A with the sequence NGFKSHALQLNNRQI (Supplementary Fig. A1). The Mascot score was reported to be 52. Serum whole complement C4 concentrations measured by enzyme-linked immunosorbent assay were not elevated in any of the 31 MS patients.
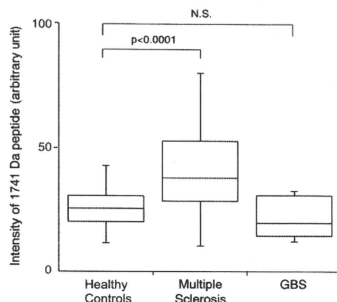

Fig. 1. The normalized intensity of the 1741-Da peptide was significantly greater in sera from patients with multiple sclerosis than in sera from healthy controls, but it was not greater in patients with Guillain–Barré syndrome (GBS) than in healthy controls.
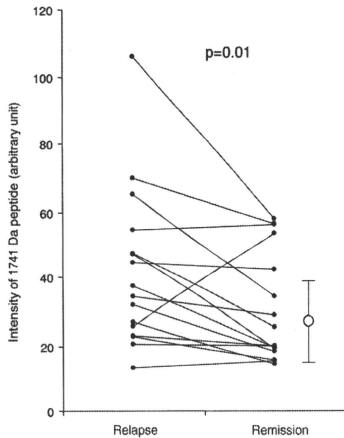
Fig. 2. Sequential changes in the normalized intensity of the 1741-Da peptide at the time of relapse compared with remission in sera from 16 patients with multiple sclerosis. There was a significant decrease during remission (Wilcoxon's test). In 13 patients, the normalized intensities were upregulated in the relapsing phase and were downregulated during remission. The open circle indicates the normal mean value, and the error bars represent the standard deviation of the normal control values.

4. Discussion

Our results showed that a fragment peptide of complement C4 was elevated in acute phase sera from MS patients. Recent advances in mass spectrometry have enabled the identification of hundreds of low-molecular-weight peptides that have previously been difficult to detect in human serum (Villanueva et al., 2006). Most of the low-molecular-weight peptides are fragments of large precursor proteins, and may reflect the results of protein interaction in the molecular pathogenesis. Novel disease markers are expected to be found from the low-molecular-weight peptides. MALDI-TOF is a key tool for analyzing clinical blood samples rapidly. Some advantages of this method are its high-throughput capability and its need of small sample sizes for analysis.

Using proteomic analyses, we identified a novel possible serum biomarker among the low-molecular-weight peptides in sera from the MS patients; this 1741-Da peptide was identified as a fragment of complement C4. Serum levels of this peptide were elevated in patients with relapsing–remitting MS at the time of relapse, whereas serum concentrations of the whole complement C4 were normal.

A previous study showed that complement C4 concentrations in MS patients are low in the CSF and are elevated in the serum (Jans et al., 1984). However, not all of the studies found like this are statistically significant. At present, there is no firm consensus concerning serum complement C4 concentrations in MS patients.

The fragment of complement C4 found in this study was possibly made during complement activation. The complement system is activated via the classical pathway, alternative pathway, and plasma protein mannose-binding lectin. Complement C4 fragmentation participates in the classical pathway and the lectin pathway. The classical pathway is primarily activated by antibody–antigen complexes. MS is considered to be a cell-mediated chronic inflammatory disease; however, B cells (Franciotta et al., 2008) and activated complement (Storch et al., 1998) were recently observed in active MS lesions. These findings raise the possibility of the association of complement with new demyelinated lesions, at least in a subgroup of MS. The lectin pathway is initiated when mannose-binding lectin binds to monosaccharides on the surface of bacteria and parasites. The infectious etiology of MS was previously discussed (Steiner et al., 2001). In the pathogenesis of MS, complement activation might occur through the classical or lectin pathway.

The possibility of the effects of some infection triggering relapse could not be excluded, but GBS patients who had obvious antecedent infection did not show increased level of 1741-Da peptide. We therefore think that our data in MS patients were not significantly affected by infection if any.

Previous studies showed that the same fragment of complement C4 found in the present study was detected in serum from patients with breast cancer (Villanueva et al., 2006) or hepatocellular carcinoma (Goldman et al., 2007). The mechanisms of action and function of this fragment are currently unknown, but our results suggest that there is a possible relationship between the fragment and the trigger of relapse in MS. Future studies are required to examine this relation longitudinally for longer periods of time in individual patients.

We emphasize on the importance of analyzing low-molecular-weight peptides that have not yet been detected by conventional techniques. Mass spectrometry may be useful in detecting small peptides and providing new insights concerning the pathophysiology of a variety of neurological disorders, including MS.

Appendix A. Supplementary data

Supplementary data associated with this article can be found, in the online version, at doi:10.1016/j.jneuroim.2009.10.019.

References

Aranami, T., Miyake, S., Yamamura, T., 2006. Differential expression of CD11c by peripheral blood NK cells reflects temporal activity of multiple sclerosis. J. Immunol. 177, 5659–5667.

Coles, A.J., Wing, M., Smith, S., Coraddu, F., Greer, S., Taylor, C., Weetman, A., Hale, G., Chatterjee, V.K., Waldmann, H., Compston, A., 1999. Pulsed monoclonal antibody treatment and autoimmune thyroid disease in multiple sclerosis. Lancet 354, 1691–1695.

Del Boccio, P., Pieragostino, D., Lugaresi, A., Di Ioia, M., Pavone, B., Travaglini, D., D'Aguanno, S., Bernardini, I., Sacchetta, P., Federici, G., Di Ilio, C., Gambi, D., Urbani, A., 2007. Cleavage of cystatin C is not associated with multiple sclerosis. Ann. Neurol. 62, 201–204.

Ebert, M.P., Niemeyer, D., Deininger, S.O., Wex, T., Knippig, C., Hoffmann, J., Sauer, J., Albrecht, W., Malfertheiner, P., Röcken, C., 2006. Identification and confirmation of increased fibrinopeptide a serum protein levels in gastric cancer sera by magnet bead assisted MALDI-TOF mass spectrometry. J. Proteome Res. 5, 2152–2158.

Franciotta, D., Salvetti, M., Lolli, F., Serafini, B., Aloisi, F., 2008. B cells and multiple sclerosis. Lancet Neurol. 7, 852–858.

Frisullo, G., Angelucci, F., Caggiula, M., Nociti, V., Iorio, R., Patanella, A.K., Sancrica, C., Mirabella, M., Tonali, P.A., Batocchi, A.P., 2006. pSTAT1, pSTAT3, and T-bet expression in peripheral blood mononuclear cells from relapsing–remitting multiple sclerosis patients correlates with disease activity. J. Neurosci. Res. 84, 1027–1036.

Frohman, E.M., Havrdova, E., Lublin, F., Barkhof, F., Achiron, A., Sharief, M.K., Stuve, O., Racke, M.K., Steinman, L., Weiner, H., Olek, M., Zivadinov, R., Corboy, J., Raine, C., Cutter, G., Richert, J., Filippi, M., 2006. Most patients with multiple sclerosis or a clinically isolated demyelinating syndrome should be treated at the time of diagnosis. Arch. Neurol. 63, 614–619.

Goldman, R., Ressom, H.W., Abdel-Hamid, M., Goldman, L., Wang, A., Varghese, R.S., An, Y., Loffredo, C.A., Drake, S.K., Eissa, S.A., Gouda, I., Ezzat, S., Moiseiwitsch, F.S., 2007. Candidate markers for the detection of hepatocellular carcinoma in low-molecular weight fraction of serum. Carcinogenesis 28, 2149–2153.

International Multiple Sclerosis Genetics Consortium, Hafler, D.A., Compston, A., Sawcer, S., Lander, E.S., Daly, M.J., De Jager, P.L., de Bakker, P.I., Gabriel, S.B., Mirel, D.B., Ivinson, A.J., Pericak-Vance, M.A., Gregory, S.G., Rioux, J.D., McCauley, J.L., Haines, J.L., Barcellos, L.F., Cree, B., Oksenberg, J.R., Hauser, S.L., 2007. Risk alleles for multiple sclerosis identified by a genomewide study. N. Engl. J. Med. 357, 851–862.

Irani, D.N., Anderson, C., Gundry, R., Cotter, R., Moore, S., Kerr, D.A., McArthur, J.C., Sacktor, N., Pardo, C.A., Jones, M., Calabresi, P.A., Nath, A., 2006. Cleavage of cystatin C in the cerebrospinal fluid of patients with multiple sclerosis. Ann. Neurol. 59, 237–247.

Jans, H., Heltberg, A., Zeeberg, I., Kristensen, J.H., Fog, T., Raun, N.E., 1984. Immune complexes and the complement factors C4 and C3 in cerebrospinal fluid and serum from patients with chronic progressive multiple sclerosis. Acta. Neurol. Scand. 69, 34–38.

Kanesaka, T., Mori, M., Hattori, T., Oki, T., Kuwabara, S., 2006. Serum matrix metalloproteinase-3 levels correlate with disease activity in relapsing–remitting multiple sclerosis. J. Neurol. Neurosurg. Psychiatry 77, 185–188.

Kappos, L., Antel, J., Comi, G., Montalban, X., O'Connor, P., Polman, C.H., Haas, T., Korn, A.A., Karlsson, G., Radue, E.W., FTY720 D2201 Study Group, 2006. Oral fingolimod (FTY720) for relapsing multiple sclerosis. N. Engl. J. Med. 355, 124–140.

Kappos, L., Bates, D., Hartung, H.P., Havrdova, E., Miller, D., Polman, C.H., Ravnborg, M., Hauser, S.L., Rudick, R.A., Weiner, H.L., O'Connor, P.W., King, J., Radue, E.W., Yousry, T., Major, E.O., Clifford, D.B., 2007. Natalizumab treatment for multiple sclerosis: recommendations for patient selection and monitoring. Lancet. Neurol. 6, 431–441.

Koning, N., Bo, L., Hoek, R.M., Huitinga, I., 2007. Downregulation of macrophage inhibitory molecules in multiple sclerosis lesions. Ann. Neurol. 62, 504–514.

Kuenz, B., Lutterotti, A., Khalil, M., Ehling, R., Gneiss, C., Deisenhammer, F., Reindl, M., Berger, T., 2005. Plasma levels of soluble adhesion molecules sPECAM-1, sP-selectin and sE-selectin are associated with relapsing–remitting disease course of multiple sclerosis. J. Neuroimmunol. 167, 143–149.

Mahad, D.J., Lawry, J., Howell, S.J., Woodroofe, M.N., 2003. Longitudinal study of chemokine receptor expression on peripheral lymphocytes in multiple sclerosis: CXCR3 upregulation is associated with relapse. Mult. Scler. 9, 189–198.

Onodera, H., Nakashima, I., Fujihara, K., Nagata, T., Itoyama, Y., 1999. Elevated plasma level of plasminogen activator inhibitor-1 (PAI-1) in patients with relapsing–remitting multiple sclerosis. Tohoku. J. Exp. Med. 189, 259–265.

Pittock, S.J., Weinshenker, B.G., Noseworthy, J.H., Lucchinetti, C.F., Keegan, M., Wingerchuk, D.M., Carter, J., Shuster, E., Rodriguez, M., 2006. Not every patient with multiple sclerosis should be treated at time of diagnosis. Arch. Neurol. 63, 611–614.

Polman, C.H., Reingold, S.C., Edan, G., Filippi, M., Hartung, H.P., Kappos, L., Lublin, F.D., Metz, L.M., McFarland, H.F., O'Connor, P.W., Sandberg-Wollheim, M., Thompson, A.J., Weinshenker, B.G., Wolinsky, J.S., 2005. Diagnostic criteria for multiple sclerosis: 2005 revisions to the "McDonald Criteria". Ann. Neurol. 58, 840–846.

Polman, C.H., O'Connor, P.W., Havrdova, E., Hutchinson, M., Kappos, L., Miller, D.H., Phillips, J.T., Lublin, F.D., Giovannoni, G., Wajgt, A., Toal, M., Lynn, F., Panzara, M.A.,

Sandrock, A.W., AFFIRM Investigators, 2006. A randomized, placebo-controlled trial of natalizumab for relapsing multiple sclerosis. N. Engl. J. Med. 354, 899–910.

Rudick, R.A., Stuart, W.H., Calabresi, P.A., Confavreux, C., Galetta, S.L., Radue, E.W., Lublin, F.D., Weinstock-Guttman, B., Wynn, D.R., Lynn, F., Panzara, M.A., Sandrock, A.W., Investigators, S.E.N.T.I.N.E.L., 2006. Natalizumab plus interferon beta-1a for relapsing multiple sclerosis. N. Engl. J. Med. 354, 911–923.

Steiner, I., Nisipianu, P., Wirguin, I., 2001. Infection and the etiology and pathogenesis of multiple sclerosis. Curr. Neurol. Neurosci. Rep. 1, 271–276.

Storch, M.K., Piddlesden, S., Haltia, M., Iivanainen, M., Morgan, P., Lassmann, H., 1998. Multiple sclerosis: in situ evidence for antibody- and complement-mediated demyelination. Ann. Neurol. 43, 465–471.

Umemura, H., Nezu, M., Kodera, Y., Satoh, M., Kimura, A., Tomonaga, T., Nomura, F., 2009. Effects of the time intervals between venipuncture and serum preparation for serum peptidome analysis by matrix-assisted laser desorption/ionization time-of-flight mass spectrometry. Clin. Chim. Acta 406, 179–180.

Villanueva, J., Shaffer, D.R., Philip, J., Chaparro, C.A., Erdjument-Bromage, H., Olshen, A.B., Fleisher, M., Lilja, H., Brogi, E., Boyd, J., Sanchez-Carbayo, M., Holland, E.C., Cordon-Cardo, C., Scher, H.I., Tempst, P., 2006. Differential exoprotease activities confer tumor-specific serum peptidome patterns. J. Clin. Invest. 116, 271–284.

Zhang, X., Leung, S.M., Morris, C.R., Shigenaga, M.K., 2004. Evaluation of a novel, integrated approach using functionalized magnetic beads, bench-top MALDI-TOF-MS with prestructured sample supports, and pattern recognition software for profiling potential biomarkers in human plasma. J. Biomol. Tech. 15, 167–175.

Efficiency of Rice Bran for Removal of Pretilachlor and Esprocarb in Artificial Gastric Fluid

Atsuko Adachi,[*,a] Yuki Okita,[a] and Jun Adachi[b]

[a]Department of Hygienic Sciences, Kobe Pharmaceutical University, Motoyamakitamachi, 4–chome, Higashinada-ku, Kobe 658–8558, Japan and [b]Graduate School of Global Environmental Studies, Kyoto Uiversity, Yoshida-Honmachi, Sakyo-ku, Kyoto 606–8501, Japan

Rice bran was found to effectively adsorb pesticides in artificial gastric fluid. Equilibrium adsorption isotherms conformed to the Freundlich type (log-log linear). Pretilachlor and esprocarb were successfully removed in artificial gastric fluid with an average removal efficiency of 85.5% and 95.8%, respectively after 90 min when rice bran (10 g/l) was added to samples containing from 0.05 to 5 mg/l of pesticides. The removal of pesticides by rice bran was attributed to the uptake by intracellular particles called spherosomes.

Key words — pretilachlor, esprocarb, spherosome, rice bran, Freundlich isotherm

INTRODUCTION

Pesticide residues in humans are mainly derived from the ingestion of contaminated food. Food is the main source of exposure of the general population to pesticides, and accounts for more than 90% of the total exposure.[1] Pesticide residues in foods and crops are a direct result of the application of pesticides to crops growing in field, and, to a lesser extent, from pesticide residues remaining in the soil.[2] There has been much interest in the use of organoclays as adsorbents to remove and remediate pesticide in contaminated agricultural soil.[3–5] Ac-

*To whom correspondence should be addressed: Department of Hygienic Sciences, Kobe Pharmaceutical University, Motoyamakitamachi, 4–chome, Higashinada-ku, Kobe 658–8558, Japan. Tel.: +81-78-441-7584; Fax: +81-78-441-7584; E-mail: a-adachi@kobepharma-u.ac.jp

tivated carbon, zeolite particles, kaolinite, fuller's earth and bentonite have been evaluated for the treatment of acute pesticide poisoning by oral ingestion.[6–9] Because of the hydrophilic character of their surfaces, clay minerals, particularly phyllosilicates, have been shown to be very good adsorbents for highly polar pesticides, but their adsorption capacity for organic compounds is usually low.[10–12] Our research has focused on the adsorption properties of rice bran.[13] The object of this work was to elucidate the effect of rice bran for removing pesticide in artificial gastric fluid.

MATERIALS AND METHODS

Apparatus —— The assay of pretilachlor or esprocarb was performed on a Shimadzu Model GC-14B gas chromatograph equipped with a flame ionization detector and a capillary column (ULBON HR-52, 30 m × 0.53 mm Shinwa Chemical ludustries, LTD., Kyoto, Japan). The column was maintained at 250°C, with both the injection port and detector were maintained at 280°C.

Materials —— Rice bran was purchased at a local market. Pretilachlor and esprocarb of analytical standard purity were purchased from Wako Pure Chemical Industries Ltd. (Amagasaki, Japan). Activated carbon (powder, coal based carbon) was purchased of practical grade from Wako Pure Chemical Industries Ltd.

Artificial Gastric Fluid —— Artificial gastric fluid was prepared by United States Pharmacopeia (USP) method.[14] Sodium chloride (2.0 g) and pepsin (3.2 g) were dissolved in hydrochloric acid (7.0 ml) and sufficient water to make 1000 ml. This solution has a pH of about 1.2.

Adsorption Experiment —— A 100 ml of sample solutions containing 0.05 or 5 mg/l of pretilachlor or esprocarb (Pesticides were dissolved in artificial gastric fluid) and rice bran (0.05–1.0 g) were placed into 100 ml glass stoppered Erlenmeyer flasks and mixed with a stirrer at 37°C. The reaction mixture was filtered through filter paper (quantitative ashless No. 5A Toyo Roshi, Ltd., Tokyo, Japan) to remove the rice bran. The initial 10 ml of filtrate was discarded because of the adsorption of pesticides by the filter paper. In control samples without rice bran, the subsequent filtrate after the discarded portion contained the same amount of adsorbent as the original solution. Fifty ml of this filtrate was

placed in a separatory funnel and 5 ml of m-xylene was added to the solution. The mixture was shaken for 1 min. The separated m-xylene layer was subjected to gas chromatography (GC) to assay the concentration of pesticides. To assess the evaporation loss of pesticides, control experiments without rice bran were performed as above. Maximum loss was about 5% (4.7 ± 0.22%), although negligible loss was detected in most cases. The removal efficiency of rice bran was calculated after taking into account the evaporation loss of pesticides. Values are shown as means ± S.D.

Recovery Test ── To determine the method efficiency for pretilachlor and esprocarb, the recovery experiments were performed following the same procedure as for the sample treatment, except for the absence of rice bran.

Isolation of Spherosomes ── Spherosomes were isolated using an improved method based on that of Moreau et al.[15] Samples of 1 g (dry weight basis) of rice bran were ground in 40 ml of grinding medium consisting of 20 mM sodium acetate, pH 5.6, containing 10 mM $CaCl_2$ with a mortar and pestle. The paste was filtered through four layers of cheesecloth, and the filtrate centrifuged at 30000 × g for 20 min. The spherosome pad was removed from the surface with a spatula and washed by resuspending in 40 ml of fresh medium. This suspension was recentrifuged at 30000 × g for 20 min. This process was repeated two more times, and the final

pellet was used as the spherosome fraction. The composition of rice bran and spherosome is shown in Table 1. Moisture content was determined by drying a sample for 6 hr at 110°C. Protein concentration was determined by the method of Kjeldahl.[16] Lipids were extracted by the Bligh and Dyer method.[17] The mass of the total lipid was determined by drying an aliquot of chloroform extract in a vacuum oven overnight and weighing the resulting lipid residue. Carbohydrate (glucide) was determined by Anthrone method.[18] Dietary fiber was determined by Association of Official Analytical Chemists (AOAC) method.[19]

RESULTS AND DISCUSSION

Recovery Studies

The recovery of pretilachlor and esprocarb can be checked according to the procedures for the recovery test. The mean recoveries of added pretilachlor and esprocarb (0.05 or 5 mg/l) in the distilled water samples were 95.1–97.1% for pretilachlor and 95.8–98.1% for esprocarb. The limit of quantification was defined for GC as the sample concentration required to give a signal-to-noise ratio of 6 : 1. It was evaluated at 0. 001 mg/l of water.

Adsorption Rate

Table 2 shows efficiencies of rice bran for the removal of pretilachlor and esprocarb in artificial gastric fluid at a reaction time of 90 min, because the removal efficiency became constant after 60 min treatment. The average removal efficiencies for pretilachlor and esprocarb was 85.5% and 95.8%, respectively. This removal efficiency was similar to that of distilled water.

Adsorption Isotherm

The amount of pretilachlor and esprocarb adsorbed in the equilibrium state was plotted against

Table 1. Composition of Rice Bran and Spherosomes

Constituent	Concentration (g/100 g)	
	Rice Bran	Spherosomes
Water	13.5	9.8
Protein	13.2	26.6
Lipid	18.3	3.9
Carbohydrate		
glucide	38.3	38.4
fiber	7.8	3.6
Ash	8.9	17.4

Table 2. Removal Efficiency of Rice Bran for Pretilachlor and Esprocarb in Artific Gastric Fluid

Substance	Concentration (mg/l)		Removal efficiency (%)
	Before treatment	After treatment	
Pretilachlor	0.05	0.005–0.007	87.2 ± 1.2[a]
	5	0.7 –0.9	83.7 ± 1.6[a]
Esprocarb	0.05	0.001–0.002	97.0 ± 0.2[a]
	5	0.2 –0.3	94.6 ± 0.9[a]

a) Data represent the mean ± S.D. of three separate determinations. Rice bran, 10 g/l; reaction time, 90 min.
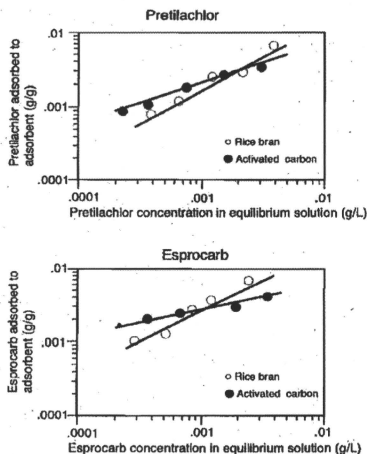
Fig. 1. Freundlich's Adsorption Isotherm of Pretilachlor and Esprocarb

Data represent the mean ± S.D. of three separate determinations. Reaction time: 3 hr, pretilachlor or esprocarb: 5 mg/l, pH: 1.2.

Fig. 2. Effect of Amount on of Rice Bran on the Adsorption of Pretilachlor and Esprocarb in Artificial Gastric Fluid

Data represent the mean ± S.D. of three separate determinations. Rice bran: (■) 1.0 g/l, (▲) 2.0 g/l, (●) 10 g/l, pretilachlor or esprocarb: 5 mg/l, pH: 1.2.

the concentration of these compounds in solution on a logarithmic scale. Equilibrium was measured after at least 3 hr of contact. A linear relationship was obtained, indicating that the adsorption reaction was of a Freundlich type (Fig. 1). This result indicated that the adsorption efficiency of rice bran for esprocarb and pretilachlor was higher than that of activated carbon in the high concentration range.

Effect of Amount of Rice Bran on Adsorption

Figure 2 shows the effect of the amount of rice bran on the removal of pretilachlor and esprocarb. The residual pesticide decreases in response to the amount of rice bran. The removal is initially fast, but after 60 min, the removal appears to plateau. In this experiment, 10 g/l of rice bran showed the highest efficiency.

Adsorption Mechanism

We investigated the mechanism of removal. We have previously reported that rice bran was effective in removal of organochlorine compounds such as chloroform, dichloromethane and benzene. Furthermore, it was confirmed that the spherosomes isolated from rice bran were effective in removing these organic compounds.[13] Analytical and laser
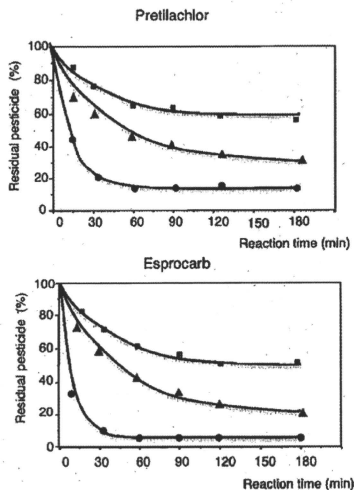
microscopic data have confirmed that the removal of organochlorine compounds and benzene is dependent on the uptake of these compounds into intracellular particles called spherosomes.[13] Spherosomes are intracellular particles about 10 μm in diameter and widely distributed among plants and fungi.[20] Neither the function of spherosomes nor its analysis is well understood.

Spherosomes are organelles rich in lipid, and they differ in morphology and origin from large oil bodies.[21] Table 3 shows the removal efficiency of pretilachlor and esprocarb by spherosomes isolated from 1 g (dry weight basis) of rice bran. The removal by spherosomes was similar to that of rice bran. We regarded the special membranes to be related to the uptake of chemical compounds into spherosomes. The chemical nature of the spherosomes is uncertain. Based on the result, we concluded that removal by rice bran is dependent on the uptake into spherosomes.

Activated carbon has usually been used for oral use as detoxification.[6] At equilibrium, the adsorption efficiency of rice bran for pretilachlor and esprocarb was higher than that of activated carbon in

Table 3. Removal Efficiency of Spherosome Isolated from Rice Bran for Pretilachlor and Esprocarb in Artificial Gastric Fluid

Substance	Concentration (mg/l)		Removal efficiency (%)
	Before treatment	After treatment	
Pretilachlor	5	1.3–1.6	71.5 ± 3.8[a]
Esprocarb	5	0.7–0.9	81.4 ± 4.6[a]

a) Data represent the mean ± S.D. of three separate determinations. All spherosomes obtained from rice bran (1 g) were used for this experiment. Reaction time, 90 min.

the high concentration range. Our study showed that the use of rice bran as an adsorbent is an efficient method for the treatment of acute pesticide poisoning by oral ingestion. Rice bran is by product of making polished rice from brown rice. Therefore, rice bran is very inexpensive, costing 1/50 – 1/40 that of activated carbon. Additionally, the use of rice bran is significant from the aspect of effective utilization of waste matter.

Taken together, the findings of this study suggest that the use of rice bran as an adsorbent is an efficient and cost-effective method for removal of pretilachlor and esprocarb in artificial gastric fluid.

REFERENCES

1) Mills, P. A. (1936) Pesticide residue content. *J. Assoc. Off. Anal. Chem.*, **46**, 762–767.

2) Businelli, A., Vischetti, C. and Coletti, A. (1992) Validation of Koc approach for modelling the fate of some herbicides in italian soil. *Fresenius Environmental Bulletin*, **1**, 583–588.

3) Mortland, M. M., Shaobai, S. and Boyd, S. S. (1986) Clay-organic complexes as adsorbents for phenol and chlorophenols. *Clays Clay Miner.*, **34**, 581–585.

4) Boyd, S. A., Mortland, M. M. and Chiou, C. T. (1988) Sorption characteristics of organic compounds on hexadecyltrimethyl ammonium-smectite. *Soil Sci. Soc. Am. J.*, **52**, 652–657.

5) Hermosin, M. C. and Comejo, J. (1993) Binding mechanism of 2,4-dichlorophenoxy acetic acid by organoclays. *J. Environ. Qual.*, **22**, 325–331.

6) Hiraishi, M. (1987) The effect of oral adsorbent on surgically induced hepatic failure. *Surg. Today*, **17**, 517–527.

7) Walcarius, A. and Mouchotte, R. (2004) Efficient in vitro paraquat removal via irreversible immobilization zeolite particles. *Arch. Environ. Contam. Toxicol.*, **46**, 135–140.

8) Keizer, A. (1990) Adsorption of paraquat ions on clay minerals. Electrophoresis of clay particles. *Prog. Colloid Polym. Sci.*, **83**, 118–126.

9) Okonek, S., Setyadharma, H., Borchert, A. and Krienke, E. G. (2005) Activated charcoal is as effective as fuller's earth or bentonite in paraquat poisoning. *J. Mol. Med.*, **60**, 207–210.

10) Jaynes, W. F. and Vance, G. F. (1996) BTEX sorption by organo-clays:cosorptive enhancement and equivalence of interlayer complexes. *Soil Sci. Soc. Am. J.*, **60**, 1742–1749.

11) Celis, R., Koskinen, M. J., Hermosin, M. C., Ulibarri, M. A. and Cornejo, J. (2000) Triadimefon interactions with organoclays and organohydrotalcites. *Soil Sci. Soc. Am. J.*, **64**, 36–43.

12) Lee, J. F., Crum, J. and Boyd, S. A. (1989) Enhanced retention of contaminants by soils exchanged with organic cations. *Environ. Sci. Technol.*, **23**, 1365–1372.

13) Adachi, A., Ikeda, C., Takagi, S., Fukao, N., Yoshie, E. and Okano, T. (2001) Efficiency of rice bran for removal of organochlorine compounds and benzene from industrial wastewater. *J. Agric. Food Chem.*, **49**, 1309–1314.

14) US Pharmacopeial Convention, Inc. (USA) (1995)

15) Moreau, R. A., Liu, K. F. and Huang, A. H. (1980) Spherosomes of castor bean endosperm. *Plant Physiol.*, **65**, 1176–1180.

16) Kjeldahl, J. (1883) Neue method zur bestimmung des stickstoffs in organischen korpern. *Ztschr Analytical Chemistry*, **33**, 366–382.

17) Bligh, E. G. and Dyer, W. J. (1959) A rapid method of total lipid extraction and purification. *Can. J. Biochem.*, **37**, 911–915.

18) Scott, T. A. and Melvin, E. H. (1952) Determination of dextran with anthrone. *Anal. Chem.*, **25**, 1656–1661.

19) Southgate, D. A. T. (1969) Determination of carbohydrates in foods. *J. Sci. Food Agric.*, **20**, 331–335.

20) Buttrose, M. S. and Ikeda, C. (1963) Ultrastructure of the developing aleurone cells of wheat grains. *J. Biol. Sci.*, **16**, 768–774.

21) Jelsema, C. L., Morre, D. J., Ruddat, M. and Turner, C. (1977) Isolation and Characterization of the lipid reserve bodies, spherosomes, from aleurone layers of wheat. *Bot. Gaz.*, **138**, 138–149.

Proteomic Analysis for the Purpose of Understanding the Mechanisms of Benzene and X-ray Induced Leukemia Using Human Bone Marrow Cells

Katsunori Sasaki[1]*, Yoshinori Nishida[1], Jun Adachi[2], Katsuya Okawa[3],
Aki Nakayama[1], Minoru Yoneda[1], Shinsuke Morisawa[1]

[1]Kyoto University Graduate School of Engeneering
[2]Kyoto University Graduate School of Global Environmental Studies
[3]Kyoto University Graduate School of Medicine

Abstract

Benzene and the ionizing radiation are well known as leukemogens. There have been many studies on leukemia accumulated, but the mechanisms underlying the leukemogenicity are not fully understood. Since there are differences and similarities in leukemogenesis by benzene and radiation, comparative analysis could offer insight toward understanding basic leukemogenesis. In this study, we extracted proteins from CD34+ cells from human bone marrow, the target organ of leukemia, exposed to benzene metabolites (catechol and hydroquinone) or/and X-rays, and performed two dimensional gel image analysis. As a result, we identified 8 proteins specific to benzene metabolites exposure, and 14 to X-ray irradiation. Notably, we found 2 proteins, protein SET and cofilin-1, which showed changes in expression levels common to both benzene metabolites and X-ray exposure. These results suggest that the SET-PP2A-JNK pathway might play a key role in the mechanisms of the leukemia.

Introduction

Benzene (C_6H_6) is an important industrial chemical. It is commonly used as an industrial solvent and synthetic material, and the main sources of exposure are cigarette smoke and exhaust gas of gasoline (Chemicals Evaluation and Research Institute (CERI), 1997). Benzene is known to cause adverse health effects on humans such as acute myelogenous leukemia. Epidemiological studies of benzene-exposed workers have demonstrated a causal relationship between benzene exposure and the induction of myelogenous leukemia (International Programme on Chemical Safety (IPCS), 1993). Among them, Pliofilm cohort study from 1970 is a sufficiently large well-studied cohort with enough benzene exposure to lead benzene risk estimation statistically. When benzene is taken into the body, it is metabolized to various metabolites by the action of metabolic enzymes such as cytochrom P-450 and myeloperoxidase (Parke, 1996). Benzene itself is a stable substance, but some of these metabolites have cytotoxicity and mutagenicity, and they are thought to contribute to the development of benzene-induced leukemia (Sammett et al., 1979). Among various metabolites, catechol (CAT) and hydroquinone (HQ) are reported to have an especially close connection with the leukemogenesis of benzene (Robertson et al., 1991). There have been many studies on benzene-induced leukemia accumulated, but the mechanisms underlying benzene-induced leukemogenicity are still not fully understood. The analysis of the effects of CAT and HQ on human bone marrow, which is the target organ of leukemia, is beneficial for getting better understanding on the mechanisms of benzene-induced leukemogenicity. In such analysis, the synergistic effects of CAT and HQ should be considered because CAT and HQ are simultaneously in bone marrow of humans and because it has reported that the combination exposure of CAT and HQ showed stronger toxicity than the individual exposure of CAT of HQ (Roberston et al., 1991; Igarashi, 2004, Kyoto University, Japan, unpublished observation; Levay and Bodell, 1991; Stillman et al., 1999).

As well as benzene, the radiation exposure causes various health effects including leukemia. It has been reported that exposure to 1Gy of radiation leads to an increasing incidence of cancers by 0.05-0.16% (Bertell, 1984). 0.1Gy of low Linear En-

ergy Transfer (LET) radiation has also been estimated to increase the carcinogenic rate by 0.5-1.4% (Committee on the Biological Effects of Ionizing Radiation (BEIR), 1980). In addition, it was shown that gene mutations could be induced artificially by X-ray exposure (Muller, 1927). X-ray is a form of electromagnetic radiation with a wavelength in the range of 0.01 to 10 nanometers. It is primarily used for medical diagnostics with the help of its high penetration. Today the exposure from medical X-rays has the highest percentage of exposure from man-made radiation. X-ray has been frequently used for biological study because the X-ray machines are easier to handle than other radiation sources.

Both benzene and radiation are similarly known to induce leukemia. They induce in common some DNA damages to human bone marrow cells, resulting in the induction of leukemia. For example, it was reported that benzene and radiation induced same kinds of chromosome aberrations such as t(8;21) and the losses of long arms or whole chromosome 5 and 7, which were thought to have some connections with leukemogenesis (McHale et al., 2008; Deininger et al., 1998; Domracheva et al., 2002). These results suggested that the inductions of leukemia by benzene and radiation exposure might have some similar mechanisms of action. However, there are also some differences. At first, there is a difference on the subtypes of leukemia induced by benzene and radiation. The relationship of benzene with acute myeloid leukemia (AML) is already proven, but there was no persuasive evidence the link of benzene to other subtypes of acute lymphocytic leukemia (ALL), chronic myeloid leukemia (CML), and chronic lymphocytic leukemia (CLL) (Schnatter et al., 2005). On the other hand, there was strong evidence of radiation-induced risks for all subtypes of leukemia (Preston et al., 1994). In addition, there have been another differences in the mechanisms of leukemia by them. In radiation-induced leukemia, DNA damages of bone marrow cells, which are the primary steps of leukemogenesis, is inducted mainly by two kinds of actions: one is the direct action in which the exposed radiation ionizes or excites the atoms constituting DNA and DNA damages are directly generated, and the other is the indirect action in which water molecules are ionized or excited by radiation and free radicals are produced, then these radicals induce DNA damages (Iida, 2009). On the other hand, in benzene-induced leukemia, DNA damages are mainly induced by binding of benzene metabolites such as CAT and HQ to intracellular molecules or by reactive oxygen species (ROSs) generated by the oxidation of benzene metabolites (Irons, 1985). It has also reported that benzene metabolites inhibit enzymes involved in DNA replication and maintenance such as topoisomerases, which are likely to contribute to benzene-induced leukemias (Eastmond et al., 2005; Lindsey et al., 2005).

Since there are differences and similarities in leukemogenesis by benzene and radiation described above, comparative analysis could give the insight of understanding basic leukemogenesis. As this comparative analysis, we conducted a comprehensive proteomic analysis by two-dimensional gel electrophoresis (2DE) using CD34+ cells from human bone marrow, which are hematopoietic stem cells and thought to be the target of leukemia.

Proteins are involved with various cancers including leukemia. Mutations on a gene level are very important as the first steps in

carcinogenesis. However, the change in protein expression alters more directly biological process than gene expressions and the essence of carcinogenesis is that mutant genes produce abnormal proteins and these proteins can not fulfill their original functions (Hirai, 1994). A translocation t(8;21) is one of the high frequency chromosome aberrations observed in acute myeloid leukemia. In this aberration, the AML1 gene on chromosome 21 and the MTG8 gene on chromosome 8 fuse together, and formed the chimera gene AML1/MTG8. The fusion protein produced by this chimera gene is regarded as a protein involved in leukemogenesis by disturbing the differentiation of myeloid cells to mature granulocytes. Additionally, one group recently reported that the primary target of radiation-induced leukemia might be not DNA itself but rather proteins (Kumagai et al., 2003; Suzuki et al., 2005; Urushibara et al., 2004). Therefore, monitoring the change of proteins may be useful as a means of getting better understanding the mechanisms underlying leukemia. Combined with the progress of analysis technology, recent researchers have actively analyzed the protein expression profile in cancers, and tumor markers are often used for the diagnosis and cure (Honda et al., 2005).

2DE is a form of gel electrophoresis commonly used for protein analysis. Using this method, we can analyze the changes of so many kinds of proteins at a time comprehensively. So, 2DE must be helpful for shedding light on the similarities and differences in leukemogenesis by benzene and radiation. Hence, we applied 2DE in this study to find proteins specific to benzene metabolites (CAT and HQ) or/and X-ray irradiation in human bone marrow cells.

Materials and Methods

Reagents and cells

Reagents were obtained from WAKO (Osaka, Japan) unless otherwise stated.

CD34+ cells used here were purchased from Lonza. (Hispanic, female, twenty six years old).

CD34+ cells were cultured at 1.3 to 2.0×105 cells/mL in StemSpan® Serum-Free Expansion Medium (SFEM) (StemCell Technolgies, Inc.) supplemented with 1% StemSpan® Cytokine Cocktail 100 (CC100) (StemCell Technologies, Inc.). The cultures were incubated in a humidified atmosphere of 5% CO_2 in air at 37 degrees C for 6 days until cultures reach early- or mid-log phase.

Chemical treatment and X-ray irradiation

For chemical treatment, the half amount of medium was exchanged for new medium after 6 days of culture, and cells were seeded at a density of $5.0×10^4$ cells/mL in a 100-mm dish and treated for 30 hr with CAT or HQ dissolved in dH_2O at the concentrations of 6 μM, or 1% of dH_2O. Cells were also treated with the mixture of CAT and HQ at the concentration of 6 μM (CAT 2 μM + HQ 4 μM). This ratio was determined according to literature, which reported the median values of CAT and HQ in the urine of exposed workers (1 to 25 ppm, n=20) were 7.2 and 16.4, 25 percentile values were 5.2 and 9.8, and 75 percentile values were 14.6 and 31.9, respectively (Rothman et al., 1998).

For X-ray irradiation, cells were re-seeded at a density of

188

1.0×10^5 cells/mL in a 50-mm dish. An X-ray exposure machine, Radioflex 350 (Rigaku, Tokyo, Japan) was used for the X-ray irradiation (5 Gy/min, 250 kV, 15 mA, Al 2 mm filter). The irradiated doses were 0, 0.5, 1 and 1.5 Gy. After irradiation, cells were cultured in the same medium for 30 hr.

Cytotoxicity analysis

Harvested cells of each treatment condition or X-ray irradiation were counted in a hematocytometer by using a phase-contrast microscope (Axiovert 25 ,Carl Zeiss, Germany). The survival rate was defined as the cell number ratio between treated cells and non-treated (control) cells. The Student's t-test was applied to test the difference of the survival rates between each dose and control.

Protein extraction

Proteins were extracted from CD34+ cells by ultrasonication using SONIFIER150 (BRANSON, Japan) directly in 100 mL of cellular lysis buffer containing 8 M urea, 4% CHAPS (GE healthcare bioscience, UK), and 40 mM Tris. Ultrasonication was conducted at 4 W for 20 sec, and after that, solutions were set on ice for 30 sec. This process was repeated five times. The suspension was centrifuged at 15000 rpm for 10 min at 4 ºC. For 2-DE, interfering components were removed using the 2-D Clean-Up Kit (GE healthcare bioscience), and proteins were diluted in cellular lysis buffer described above. The protein concentration was determined using the 2-D Quant Kit (GE healthcare bioscience). The coefficients of variation of these extraction processes were less than 15% (n = 5 per exposure condition).

2DE

For 2DE, we used 50 μg of proteins per gel. 2DE was performed in the following method.

Proteins were resuspended in 450 μL of buffer containing 8 M urea, 4% CHAPS, 40 mM Tris, 0.28% DTT (GE healthcare bioscience), and 0.5% immobilized pH gradient (IPG) buffer (GE healthcare bioscience). IPG gel strips (24 cm, pH 4-7, GE healthcare bioscience) were rehydrated with samples for 2DE using Immobiline DryStrip Reswelling Tray (GE healthcare bioscience) for 16 hr at room temperature. In order to avoid drying during the rehydration, DryStrip cover fluid (GE healthcare bioscience) was piled up on the strips. After the rehydration, isoelectric focusing (IEF) was performed with an Ettan IPGphor II instrument unit (GE healthcare bioscience) for a total of 46.9 kVh at room temperature. The detailed conditions for IEF is 1 hr at 100 V, 1 hr at 500 V, gradually increased to 1000 V over 7 hr, then gradually increased to 8000 V over 3 hr, and finally run at 8000 V for 3.45 hr.

Before the second dimensional separation, each focused IPG strip was equilibrated, firstly in a buffer (50mM Tris-HCl, 6M urea, 30% glycerol, 2% SDS, 0.002% bromophenol blue (MP biomedicals), pH8.8) containing 1% DTT for 15 min, and then in the same equilibration buffer containing 2.5% iodoacetamide for another 15 min. Both incubations were carried out at room temperature with gentle shaking using MULTI SHAKER MMS (EYELA, Japan). In this equilibration process, DTT cut the disulfide bindings in proteins, and iodoacetamide protected the exposed cysteine residues to hold primary structures of proteins. The second dimension, sodium dodecyl sulfate - poly-acryl-

amide gel electrophoresis (SDS-PAGE), was carried out using an Ettan Dalt six (GE healthcare bioscience). The upper buffer chamber of Ettan Dalt six was filled with a SDS buffer I containing 50 mM Tris, 384 mM Glycine (MP Biomedicals), and 0.2% SDS. The lower buffer chamber was filled with a SDS buffer II containing 25 mM Tris, 192 mM Glycine, and 0.1% SDS. The equilibrated IPG strips were loaded on 12.5% gels (255 mm × 205 mm × 1 mm) at 10 ºC, which contained 25% 40(w/v)%-Acrylamide/Bis Mixed Solution (37.5:1) (nacalai tesque, Kyoto, Japan), 375 mM Tris-HCl, 0.1% SDS, 0.05% ammonium persulphate (nacalai tesque), and 0.33 μL/mL TEMED (nacalai tesque). The agarose solution (0.5% agarose and 0.002% bromophenol blue in a SDS buffer II described above) was applied to seal the IPG strips, then SDS-PAGE was run at 2.5 W/gel for 30 min, followed by 25 W/gel until the bromophenol blue reached the bottom of the gel. A constant-temperature unit, NCB-2500 (EYELA) was used in order to keep the gels and buffers at 10 ºC. After SDS-PAGE, analytic gels were stained by silver staining using 2-D silver staining kit II (Daiichi, Japan).

Identification of specific proteins

For image analysis, all the silver-stained gels were scanned by image scanner GT-X 8000 (SEIKO EPSON Corporation, Japan). Electronic gel images were exported as tagged image format (TIF) in 8-bit black-and-white color with 160 μm of pixels. Images were analyzed using the PDQuest software (Bio-Rad Laboratories, Inc., USA). Twenty-four TIF images obtained from experiments (2 images from 2 treatment conditions as 0.5 Gy and 1.0 Gy, and 3 images from other 6 treatment conditions, i.e., control, CAT, HQ, CAT+HQ, 0Gy, 1.5 Gy) were loaded into the program and grouped. Spot detections were carried out automatically, followed by the manual editing of each image to remove artifacts such as streaks and splotches. All the spots on the gels were matched either automatically or manually. After each matching, the background subtraction and spot volume normalization were performed. We used the local regression model for the normalization because it is not easily affected by abnormal values. In this normalization method the variance of each spot volume was minimized. Using normalized volume as a parameter, the spots showing at least twofold changes in expression levels were identified.

For the spots specific to benzene metabolites exposure, mass spectrometric identification of proteins was performed as previously described (Jensen et al., 1996). Briefly, after SDS-PAGE, proteins were visualized by silver staining and excised separately from gels, followed by the in-gel digestions with trypsin (Promega Corporation) in a buffer containing 50mM ammonium bicarbonate (pH 8.0) and 2% acetonitrile overnight at 37 degrees C. Molecular mass analyses of tryptic peptides were performed by matrix-assisted laser desorption/ionization time-of flight mass spectrometry (MALDI-TOF/MS) using an ultraflex TOF/ TOF (Bruker Daltonics). Proteins were identified by comparison between the molecular weights determined by MALDI-TOF/MS and theoretical peptide masses from the proteins registered in NCBInr.

For the spots specific to X-ray irradiation, mass spectrometric identification of proteins was performed as follows. The gels were subjected to in-gel tryptic digestion essentially as described (Wilm et al., 1996). Briefly, the gel pieces were destained and

washed, and, after dithiothreitol reduction and iodoacetamide alkylation, the proteins were digested with porcine trypsin (mass spec grade) overnight at 37 degrees C. The resulting tryptic peptides were extracted from the gel pieces with 30% acetonitrile, 0.3% trifluoroacetic acid and 100% acetonitrile. The extracts were evaporated in a vacuum centrifuge to remove organic solvent, then desalted and concentrated on reversed-phase C18 StageTips as previously described (Rappsilber et al., 2003). Then, Nanoflow-Liquid Chromatography (LC)-MS and MS/MS experiments were performed on HITACHI Nano LC (HITACHI, Tokyo, Japan) and Q-Tof Ultima API (Waters, Milford, USA). Chromatographic separation of the peptides took place in a 10 cm fused silica column (50 μm inner diameter) in-house packed with reversed-phase ReproSil-Pur C_{18}-AQ 3 μm resin (Dr. Maisch GmbH, Ammerbuch-Entringen, Germany). Peptide mixtures were injected onto the column with a flow of 200 nl/min and subsequently eluted with a flow of 200 nl/min from 3.8% to 11.6% acetonitrile in 0.5% acetic acid, in a 5 min gradient, from 11.6 % to 26 %, in a 15 min gradient, and from 26% to 69.2%, in a 10 min gradient. Data were acquired in MS mode and data-dependent analysis (DDA) mode using MassLynx software (Waters, Milfold, USA). Proteins were identified via automated database searching (Mascot; Matrix Science, London, United Kingdom) of all tandem mass spectra against an MSIPI database (versions 3.53; European Bioinformatics Institute, www.ebi.ac.uk/IPI/msipi.html). Carbamidomethyl cysteine was set as fixed modification, and oxidized methionine and deamidation of asparagine and glutamine were searched as variable modifications. Initial mass tolerances for protein identification on MS peaks were 100 ppm and on MS/MS peaks were 0.3 Da. Two "missed cleavages" were allowed. The instrument setting for the Mascot search was specified as "ESI-QUAD-TOF". Peptides and proteins were identified using criteria as follows. Peptides which MS2 scores were above the 95th percentile of significant (Mascot score > XX). Only fully tryptic peptides with 6 amino acids or longer were accepted for identification. Proteins were considered positively identified when they were identified at least two fully tryptic peptides.

Results

Cytotoxicity analysis

Figure 1 shows the survival rates of cells in each treatment condition. The experiments on benzene metabolites were performed thrice, and those on X-ray were performed five times. In Figure 1, error bars were set based on the standard deviations. For chemical exposure, CAT treatment lowered the survival rate to 83.9%, HQ to 84.9%, and CAT+HQ to 69.2%, respectively. CAT and CAT+HQ showed significant decrease in the survival rate of cells (P < 0.05), but HQ did not show significant decrease (P = 0.106). The X-ray irradiation induced dose-response decrease in the survival rate significantly (P < 0.01). 0.5 Gy X-ray lowered the survival rate to 78.9%, 1.0 Gy to 65.2%, and 1.5 Gy to 49.0%, respectively.

2D gel image analysis

Figure 2 shows representative image (control) of silver stained 2D gels obtained from benzene metabolites treatment, and Figure 3 shows representative image (1.5 Gy) of 2D gels from X-ray irradiation. By the image analysis software, over thousand spots per gel were detected in samples, but some of them were too small or faint to be identified, so we manually selected spots enough large and deep to be quantified and identified. As a result, 692 spots per gel were detected in chemical exposure samples and 412 spots per gel were detected in X-ray irradiation samples.

Before the differential analysis, the correlation coefficients between gels were calculated based on normalized volume of each spot in order to check the reproducibility of 2DE. The Calculated values of correlation coefficients are shown in Table 1 and Table 2. Since the total amount of proteins in every gel is equal (50 mg) and the expression levels of most of the proteins remain constant across treatments, so the correlation coefficients between gels are expected to be high. As shown in Table 1 and Table 2, calculated coefficients were large enough (0.695 to 0.930) to enable us to perform differential analysis and to confirm the reproducibility of the experiments.
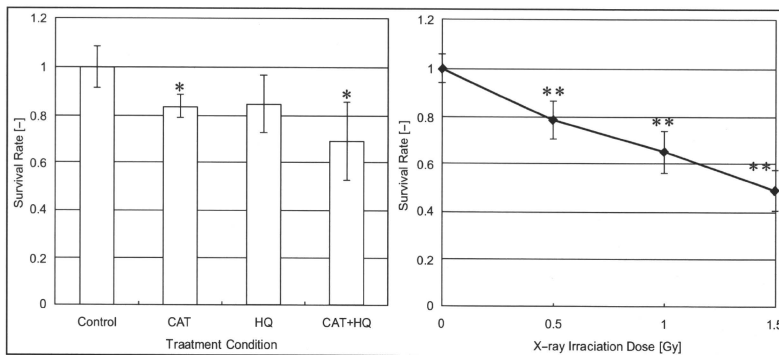

Figure 1: The survival rates of cells in chemical treatment (left) and X-ray irradiation (right). The marks * and ** mean the significance of difference (*: P < 0.05, **: P < 0.01) between control and each treatment tested by the Student's t-test.

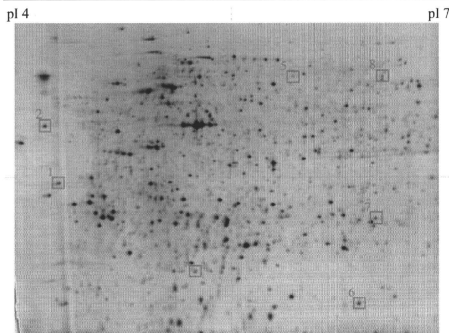pl 4   pl 7

Figure 2: Representative image of gels from benzene metabolites exposure (control). Fifty micrograms of proteins were applied to a pH 3-7 IPG strip (24cm), and with 12.5% constant vertical SDS-PAGE as the second dimension. The gel was visualized by silver staining, and the resulting image was analyzed by PDQuest software. Marked squares show specific spots to exposure.

pl 4   pl 7

Figure 3: Representative image of gels from X-ray irradiation (1.5Gy). Fifty micrograms of proteins were applied to a pH 3-7 IPG strip (24cm), and with 12.5% constant vertical SDS-PAGE as the second dimension. The gel was visualized by silver staining, and the resulting image was analyzed by PDQuest software. Marked squares show specific spots to exposure.
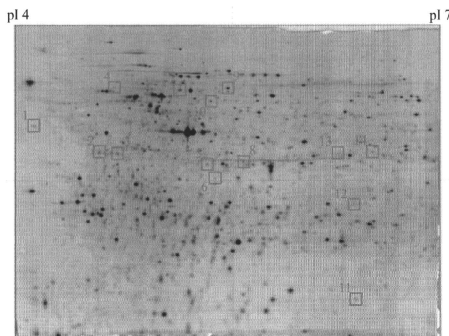
For the chemical exposure samples, the comparison was performed between the expression levels of proteins in control gels and those in treated gels. For the X-ray irradiation samples, the comparison was performed between the expression levels in 0 Gy gels and those in irradiated gels. The expression levels used for the comparison were the average of expression levels in two or three gels of the same treatment. As a result of differential analysis, we found 8 spots showing at least twofold changes in expression levels by treatment of CAT, HQ or the mixture of them. Also, 14 spots showed more than twofold changes in expression levels by X-ray irradiation. These spots were labeled in Figure 2 and Figure 3. Their expression ratios to control were shown in Table 3. We could not identify some spots specific to X-ray shown as "not identified" in Table 3 because the amounts of these proteins were too low.

Among these specific spots, two proteins, protein SET and

cofilin-1, changed their expression levels by both benzene metabolites exposure and X-ray irradiation. The expression of protein SET was decreased by HQ and X-ray exposure, and that of cofilin-1 was decreased by CAT and X-ray exposure.

Discussions

In this study, we extracted proteins from human bone marrow CD34+ cells and performed 2-D gel image analysis. As a result, we found 8 proteins specific to benzene metabolites exposure, and 14 to X-ray irradiation. Especially, we found 2 proteins, protein SET and cofilin-1, where changes common to both benzene metabolites and X-ray exposure were identified. The expression of protein SET was decreased by HQ and X-ray exposure, and that of cofilin-1 was decreased by CAT and X-ray exposure.

Cofilin-1, 18 kD phosphoprotein (p18), controls reversibly actin polymerization and depolymerization. In benign prostatic hyperplasia cells (BPH), LIM kinase 1 (LIMK1) was reported to inactivate phosphorylation of cofilin and result in chromosomal abnormalities, which indicated carcinogenicity in prostate (Davila et al., 2007; Nakano et al., 2003; Pope et al., 2004; Sumi et al., 2006).

Protein SET is a multitasking protein, involved in apoptosis, transcription, nucleosome assembly and histone binding. SET also works as a stimulator for DNA replication of the adenovirus genome complexed with viral core proteins. SET is known as a myeloid leukemia-associated protein, and it was reported that a fusion-protein, SET-CAN, was found in cases of acute undifferentiated leukemia (Adachi et al., 1994; Nagata et al., 1995; Tsujio et al., 2005; von Lindern et al., 1992). In addition, this protein is an inhibitor of protein phosphatase 2A (PP2A) and is thought to play a key role in leukemogenesis by its nuclear localization, protein-protein interactions and PP2A inhibitory activity (Minakuchi et al., 2001). PP2A is a serine/threonine phosphatase and it was reported that the activation of PP2A inhibited the activity of c-Jun N-terminal kinase (JNK), which is thought to play a key role in the control of apoptotic cell death (Shanley et al., 2001). It was also suggested that PP2A be involved in the function of cyclin G which controls the cell cycle and is known to be regulated at the transcriptional level by p53 (Li et al., 2009). Therefore, the decrease of the expression level of SET in this study might imply the excess expression of PP2A, resulting in some troubles in cell cycle such as apoptotic process. Moreover, it was reported that SET suppressed activation of ERK following EGF stimulation, which suggested that SET negatively regulates cell growth by inhibiting the G1/S transition and inhibiting the MEK/ERK pathway stimulated by external stimuli and that SET potentially functions as a tumor suppressor (Fukukawa et al., 2005). Hence, we think that there might be some problems in the control of cell cycle of bone marrow cells because of the decrease of SET by benzene metabolites and X-ray exposure, which suggests that the SET-PP2A-JNK pathway might play an important role in basic leukemogenicity.

In addition, we should pay attention to another two proteins. One is the serine/threonine-protein kinase PAK2, which was specific to the exposure of benzene metabolites, and the other is the COP9 signalosome subunit 5 (COPS5), which was specific to the X-ray exposure. PAK2 is an activated kinase acts on a variety of targets such as phosphorylates ribosomal protein S6, histone H4

gels	CON1	CON2	CON3	CAT1	CAT2	CAT3	HQ1	HQ2	HQ3	MIX1	MIX2	MIX3
CON1		0.796	0.799	0.743	0.802	0.729	0.781	0.704	0.695	0.834	0.815	0.768
CON2			0.874	0.780	0.878	0.826	0.813	0.807	0.789	0.867	0.857	0.855
CON3				0.846	0.883	0.848	0.830	0.841	0.804	0.868	0.851	0.912
CAT1					0.802	0.784	0.747	0.783	0.754	0.775	0.749	0.829
CAT2						0.847	0.829	0.821	0.788	0.877	0.861	0.858
CAT3							0.792	0.855	0.770	0.831	0.798	0.829
HQ1								0.764	0.776	0.851	0.836	0.824
HQ2									0.808	0.779	0.758	0.825
HQ3										0.777	0.763	0.797
MIX1											0.907	0.857
MIX2												0.839
MIX3												

* 'CON' means control (non-treated), 'MIX' means CAT+HQ.

Table 1: Correlation coefficients between gels of chemical exposure samples.

gels	CON1	CON2	CON3	CAT1	CAT2	CAT3	HQ1	HQ2	HQ3	MIX1	MIX2	MIX3
CON1		0.796	0.799	0.743	0.802	0.729	0.781	0.704	0.695	0.834	0.815	0.768
CON2			0.874	0.780	0.878	0.826	0.813	0.807	0.789	0.867	0.857	0.855
CON3				0.846	0.883	0.848	0.830	0.841	0.804	0.868	0.851	0.912
CAT1					0.802	0.784	0.747	0.783	0.754	0.775	0.749	0.829
CAT2						0.847	0.829	0.821	0.788	0.877	0.861	0.858
CAT3							0.792	0.855	0.770	0.831	0.798	0.829
HQ1								0.764	0.776	0.851	0.836	0.824
HQ2									0.808	0.779	0.758	0.825
HQ3										0.777	0.763	0.797
MIX1											0.907	0.857
MIX2												0.839
MIX3												

Table 2: Correlation coefficients between gels of X-ray irradiation samples.

Spot in Fig 2	Spot in Fig 3	Protein	ratio of expression level							
			CON	CAT	HQ	MIX	0Gy	0.5Gy	1.0Gy	1.5Gy
1	-	Clathrin, light polypeptide A	1	0.50	0.55	0.75	1	not specific		
2	1	Protein SET	1	0.71	0.38[c]	0.80	1	0.47	0.46	0.44
3	-	Keratin-9	1	3.06	2.42	1.50	1	not specific		
4	-	Chromobox homolog 3	1	0.79	0.23[b]	0.81	1	not specific		
5	-	Serine/threonine-protein kinase PAK2	1	1.84	4.47	1.43	1	not specific		
6	11	Cofilin-1	1	0.51	0.85	1.62	1	1.21	0.93	0.32
7	-	Proteasome subunit alpha type-6	1	1.71	2.58[c]	1.38	1	not specific		
8	-	T-complex protein 1 subunit zeta	1	1.81	2.58[a]	0.98	1	not specific		
-	2	Isoform 1 of Protein SET	1	not specific			1	0.49	0.70	0.52
-	3	40s ribosomal protein SA	1	not specific			1	0.99	0.70	0.54
-	4	not identified	1	not specific			1	0.48	0.56	0.49
-	5	highly similar to Actin, cytoplasmic 1	1	not specific			1	0.60	0.55	0.55
-	6	not identified	1	not specific			1	0.36	0.30	0.43
-	7	not identified	1	not specific			1	0.73	0.34[d]	0.69
-	8	CAPZA2 20kDa protein	1	not specific			1	0.56	0.50	0.32[e]
-	9	not identified	1	not specific			1	1.08	0.89	0.38
-	10	not identified	1	not specific			1	1.37	2.04	4.08[a]
-	12	not identified	1	not specific			1	0.33	0.72	0.44
-	13	COP9 signalosome subunit 5 variant	1	not specific			1	0.43	0.36	0.65
-	14	not identified	1	not specific			1	0.69	0.72	0.67

* 'CON' means control (non-treated), 'MIX' means CAT+HQ.
** a, b, c and d mean the significance of difference (a: P < 0.01, b: P < 0.02, c: P < 0.05, d: P < 0.1) between control and each treatment tested by the Student's t-test.
*** 'not identified' means the spots which we could not identify because the expression levels of them were too low.

Table 3: Expression levels of specific proteins and results of identification.

and myelin basic protein. This protein stimulates cell survival and cell growth. The process is, at least in part, mediated by phosphorylation and inhibition of pro-apoptotic BAD. Caspase-activated PAK2 is involved in cell death response, probably involving the JNK signaling pathway (Benner et al., 1995; 38. Rudel and Bokoch, 1997; Jakobi et al., 2003; Vilas et al., 2006). COPS5 is a probable protease subunit of the COP9 signalosome complex (CSN), a complex involved in various cellular and developmental processes. The CSN complex is an essential regulator of the ubiquitin (Ubl) conjugation pathway by mediating the deneddylation of the cullin subunits of the SCF-type E3 ligase complexes, leading to decrease the Ubl ligase activity of SCF-type complexes sugh as SCF, CSA or DDB2. The complex is also involved in phosphorylation of p53/TP53, c-jun/JUN, Ikappabalpha/NFKBIA, ITPK1 and ICSBP, possibly via its association with CK2 and PKD kinases. CSN-dependent phosphorylation of TP53 and JUN promotes and protects degradation by the Ubl system, respectively (Dechend et al., 1999; Bech-Otschir et al., 2001; Groisman et al., 2003; Uhle et al., 2003; Kim et al., 2004; Fang et al., 2008). As above, both PAK2 and COPS5 have a possible connection with the JNK signaling pathway as well as SET. Therefore, the changes of their expression levels might also suggest an important role of the SET-PP2A-JNK pathway in leukemogenicity.

While we obtained some proteins that might shed light on the leukemogenesis and might be candidates for biomarkers of leukemia, there were also some problems to be solved. Some of specific proteins detected did not show significant difference of expression levels. Moreover, in X-ray irradiated samples, there were no dose-response decrease of expression levels of proteins detected. These problems occurred mainly because the sample size was small and the variability was still a little large. To solve these problems, additional experiments with larger sample size should be conducted. Besides, more quantitative analysis such as Western blot helps to validate the change of protein expression.

Conclusions

In this study we performed 2-D gel electrophoresis using human bone marrow CD34+ cells for the purpose of finding proteins specific to benzene metabolites and/or X-ray. As a result, we found 8 proteins specific to benzene metabolites exposure and 14 to X-ray irradiation, which suggest that the SET-PP2A-JNK pathway might play a key role in the mechanisms of the leukemia.

Indeed comprehensive proteomic analyses using 2DE such as this study are useful in obtaining information for the better understanding of the unclear mechanisms of various diseases. However, it is also true that 2DE lacks the quantitative accuracy and that the validation of the results is necessary. Therefore, more quantitative analyses such as Western blot are needed in order to validate the changes of protein expressions identified in this study. In addition, further approaches such as dose-response analysis designed to include more than two exposure conditions, proteomic analysis on other leukemogens, and gene analysis as represented by DNA microarray will shed more light on the leukemogenesis.

References

1. Adachi Y, Pavlakis GN, Copeland TD (1994) Identification and characteriza-tion of SET, a nuclear phosphoprotein encoded by the translocation break point in acute undifferentiated leukemia. J Biol Chem 269: 2258-62. » CrossRef » PubMed » Google Scholar

2. Bech-Otschir D, Kraft R, Huang X, Henklein P, Kapelari B, et al. (2001) COP9 signalosome-specific phosphorylation targets p53 to degradation by the ubiquitin system. EMBO J 20: 1630-9. » CrossRef » PubMed » Google Scholar

3. BEIR (1980) The effects on populations of exposure to low levels of ion-izing radiation. Washington D. C., USA: National Academy Press. » CrossRef » PubMed » Google Scholar

4. Benner GE, Dennis PB, Masaracchia RA (1995) Activation of an S6/H4 ki-nase (PAK 65) from human placenta by intramolecular and intermolecular autophosphorylation. J Biol Chem 270: 21121-8. » CrossRef » PubMed » Google Scholar

5. Bertell R (1984) Handbook for estimation health effects from exposure to ionizing radiation. Toronto, Canada: Institute of Concern for Public Health. » CrossRef » PubMed » Google Scholar

6. CERI (1997) Chemical Substances Hazard Assessment Report: Benzene. Available at: http://qsar.cerij.or.jp/SHEET/F96_01.pdf. Accessed on 6 Oc-tober, 2009. » CrossRef » PubMed » Google Scholar

7. Davila M, Jhala D, Ghosh D, Grizzle WE, Chakrabarti R (2007) Expression of LIM kinase 1 is associated with reversible G1/S phase arrest, chromo-somal instability and prostate cancer. Mol Cancer 6: 40. » CrossRef » PubMed

8. Dechend R, Hirano F, Lehmann K, Heissmeyer V, Ansieau S, et al. (1999) The Bcl-3 oncoprotein acts as a bridging factor between NF-kappaB/Rel and nuclear co-regulators. Oncogene 18: 3316-23. » CrossRef » PubMed » Google Scholar

9. Deininger MW, Bose S, Gora-Tybor J, Yan XH, Goldman JM, et al. (1998) Selective induction of leukemia-associated fusion genes by high-dose ion-izing radiation. Cancer Res 58: 421-5. » CrossRef » PubMed » Google Scholar

10. Domracheva EV, Aseeva EA, Udovichenko AI, Obukhova TN, Ol'shanskaia IuV, et al. (2002) Induced leukemias and their connection with radiation ex-posure. Radiats Biol Radioecol 42: 715-9. » CrossRef » PubMed » Google Scholar

11. Eastmond DA, Mondrala ST, Hasegawa L (2005) Topoisomerase II inhi-bition by myeloperoxidase-activated hydroquinone: a potential mechanism underlying the genotoxic and carcinogenic effects of benzene. Chem Biol Interact 153-4: 207-16. » CrossRef » PubMed » Google Scholar

12. Eastmond DA, Mondrala ST, Hasegawa L (2008) Characterization of the hu-man COP9 signalosome complex using affinity purification and mass spec-trometry. J Proteome Res 7: 4914-25. » CrossRef » PubMed » Google Scholar

13. Fukakawa C, Shima H, Tanuma N, Okada T, Kato N, et al. (2005) The onco-protein I-2PP2A/SET negatively regulates the MEK/ERK pathway and cell proliferation. Int J Oncol 26: 751-6. » CrossRef » PubMed » Google Scholar

14. Groisman R, Polanowska J, Kuraoka I, Sawada J, Saijo M, et al. (2003) The ubiquitin ligase activity in the DDB2 and CSA complexes is differentially regulated by the COP9 signalosome in response to DNA damage. CELL 113: 357-67. » CrossRef » PubMed » Google Scholar

15. Hirai H (1994) Hakketsubyo no Bunshiigaku. Tokyo, Japan: Yodosha. » CrossRef » PubMed » Google Scholar

16. Honda T, Tamura G, Endoh Y, Nishizuka S, Kawata S, et al. (2005) Ex-pression of Tumor Suppressor and Tumor-related Proteins in Differenti-ated Carcinoma, Undifferentiated Carcinoma with Tubular Component and Pure Undifferentiated Carcinoma of the Stomach. Jpn J Clin Oncol 35: 53. » CrossRef » PubMed » Google Scholar

17. Iida H (2009) Hoshasen Gairon. Tokyo, Japan: Tsusyo Sangyo Kenkyusha. » CrossRef » PubMed » Google Scholar

18. IPCS (1993) Environmental Health Criteria 150: Benzene. Available at: http://www.inchem.org/documents/ehc/ehc/ehc150.htm. Accessed on 1 May, 2009. » CrossRef » PubMed » Google Scholar

19. Irons RD (1985) Quinones as toxic metabolites of benzene. J Toxicol Envi-ron Health 16: 673-8. » CrossRef » PubMed » Google Scholar

20. Jakobi R, McCarthy CC, Koeppel MA, Stringer DK (2003) Caspase-activat-ed PAK-2 is regulated by subcellular targeting and proteasomal degradation. J Biol Chem 278: 38675-85. » CrossRef » PubMed » Google Scholar

21. Jensen ON, Podtelejnikov A, Mann M (1996) Delayed extraction improves specificity in database searches by matrix-assisted laser desorption/ionization peptide maps. Rapid Commun Mass Spectrom 10: 1371-8. » CrossRef » PubMed » Google Scholar

22. Kim BC, Lee HJ, Park SH, Lee SR, Karpova TS, et al. (2004) Jab1/CSN5, a component of the COP9 signalosome, regulates transforming growth factor beta signaling by binding to Smad7 and promoting its degradation. Mol Cell Biol 24: 2251-62. » CrossRef » PubMed » Google Scholar

23. Kumagai J, Masui K, Itagaki Y, Shiotani M, Kodama S, et al. (2003) Long-lived mutagenic radicals induced in mammalian cells by ionizing radiation are mainly localized to proteins. Radiat Res 160: 95-102. » CrossRef » PubMed » Google Scholar

24. Levay G, Bodell WJ (1992) Potentiation of DNA adduct formation in HL-60 cells by combinations of benzene metabolites. Proc Natl Acad Sci USA 89: 7105-9. » CrossRef » PubMed » Google Scholar

25. Li H, Okamoto K, Peart MJ, Prives C (2009) Lysine-independent turnover of cyclin G1 can be stabilized by B'alpha subunits of protein phosphatase 2A. Mol Cell Biol 29: 919-28. » CrossRef » PubMed » Google Scholar

26. Lindsey RH, Bender RP, Osheroff N (2005) Stimulation of topoisomerase II-mediated DNA cleavage by benzene metabolites. Chem Biol Interact 153-4: 197-205. » CrossRef » PubMed » Google Scholar

27. McHale CM, Lan Q, Corso C, Li G, Zhang L, et al. (2008) Chromosome translocations in workers exposed to benzene. J Natl Cancer Inst Monogr 39: 74-7. » CrossRef » PubMed » Google Scholar

28. Minakuchi M, Kakazu N, Gorrin-Rivas MJ, Abe T, Copeland TD, et al. (2001) Identification and characterization of SEB, a novel protein that binds to the acute undifferentiated leukemia-associated protine SET. Eur J Biochem 268: 1340-51. » CrossRef » PubMed » Google Scholar

29. Muller HJ (1927) Artificial Transmutation of the Gene. Science 66: 84-7. » CrossRef » PubMed » Google Scholar

30. Nagata K, Kawase H, Handa H, Yano K, Yamasaki M, et al. (1995) Replication factor encoded by a putative oncogene, set, associated with myeloid leukemogenesis. Proc Natl Acad Sci USA 92: 4279-83. » CrossRef » PubMed » Google Scholar

31. Nakano K, Kanai-Azuma M, Kanai Y, Moriyama K, Yazaki K, et al. (2003) Cofilin phosphorylation and actin polymerization by NRK/NESK, a member of the germinal center kinase family. Exp Cell Res 287: 219-27. » CrossRef » PubMed » Google Scholar

32. Parke DV (1996) Personal reflections on 50 years of study of benzene toxicology. Environ Health Perspect 104: 1123-8. » CrossRef » PubMed » Google Scholar

33. Pope BJ, Zierler-Gould KM, Kühne R, Weeds AG, Ball LJ (2004) Solution structure of human cofilin: actin binding, pH sensitivity, and relationship to actin-depolymerizing factor. J Biol Chem 279: 4840-8. » CrossRef » PubMed » Google Scholar

34. Preston DL, Kusumi S, Tomonaga M, Izumi S, Ron E, et al. (1994) Cancer incidence in atomic bomb survivors. Part III. Leukemia, lymphoma and multiple myeloma, 1950-1987. Radiat Res 137: S68-97. » CrossRef » PubMed » Google Scholar

35. Rappsilber J, Ishihama Y, Mann M (2003) Stop and go extraction tips for matrix-assisted laser desorption/ionization, nanoelectrospray, and LC/MS sample pretreatment in proteomics. Anal Chem 75: 663-70. » CrossRef » PubMed » Google Scholar

36. Robertson ML, Eastmond DA, Smith M (1991) Two benzene metabolites

catechol and hydroquinone produce a synergistic induction of micronuclei and toxicity in cultured human lymphocytes. Mutat Res 249: 201-9. » CrossRef » PubMed » Google Scholar

37. Rothman N, Bechtold WE, Yin SN, Dosemeci M, Li GL, et al. (1998) Urinary excretion of phenol, Catechol, hydroquinone, and muconic acid by workers occupationally exposed to benzene. Occup Environ Med 55: 705-11. » CrossRef » PubMed » Google Scholar

38. Rudel T, Bokoch GM (1997) Membrane and morphological changes in apoptotic cells regulated by caspase-mediated activation of PAK2. Science 276: 1571-4. » CrossRef » PubMed » Google Scholar

39. Sammett D, Lee EW, Kocsis JJ, Snyder R (1979) Partial hepatectomy reduces both metabolism and toxicity of benzene. J Toxicol Environ Health 5: 785-92. » CrossRef » PubMed » Google Scholar

40. Schnatter AR, Rosamilia K, Wojcik NC (2005) Review of the literature on benzene exposure and leukemia subtypes. Chem Biol Interact 153-4: 9-21. » CrossRef » PubMed » Google Scholar

41. Shanley TP, Vasi N, Denenberg A, Wong HR (2001) The serine/threonine phosphatase, PP2A: endogenous regulator of inflammatory cell signaling. J Immunol 166: 966-72. » CrossRef » PubMed » Google Scholar

42. Stillman WS, Varella-Garcia M, Irons RD (1999) The benzene metabolites hydroquinone and catechol act in synergy to induce dose-dependent hypoploidy and -5q31 in a human cell line. Leuk Lymphoma 35: 269-81. » CrossRef » PubMed » Google Scholar

43. Sumi T, Hashigasako A, Matsumoto K, Nakamura T (2006) Different activity regulation and subcellular localization of LIMK1 and LIMK2 during cell cycle transition. Exp Cell Res 312: 1021-30. » CrossRef » PubMed » Google Scholar

44. Suzuki M, Suzuki K, Kodama S, Watanabe M (2005) Interstitial chromatin alteration causes persistens p53 activation involved in the radiation-induced senescence-like growth arrest. Biochem Biophys Res Commun 340: 145-50. » CrossRef » PubMed » Google Scholar

45. Tsujio I, Zaidi T, Xu J, Kotula L, Grundke-Iqbal I, et al. (2005) Inhibitors of proteins phosphatase-2A from human brain structures, immunocytological localization and activities towards dephosphorylation of the Alzheimer type hyperohorylated tau. FEBS Lett 579: 363-72. » CrossRef » PubMed » Google Scholar

46. Uhle S, Medalia O, Waldron R, Dumdey R, Henklein P, et al. (2003) Protein kinase CK2 and protein kinase D are associated with the COP9 signalosome. EMBO J 22: 1302-12. » CrossRef » PubMed » Google Scholar

47. Urushibara A, Kodama S, Suzuki K, Desa MB, Suzuki F, et al. (2004) Involvement of telomere dysfunction in the induction of genomic instability by radiation in scid mouse cells. Biochem Biophys Res Commun 313: 1037-43. » CrossRef » PubMed » Google Scholar

48. Vilas GL, Corvi MM, Plummer GJ, Seime AM, Lambkin GR, et al. (2006) Posttranslational myristoylation of caspase-activated p21-activated protein kinase 2 (PAK2) potentiates late apoptotic events. Proc Natl Acad Sci USA 103: 6542-7. » CrossRef » PubMed » Google Scholar

49. von Lindern M, van Baal S, Wiegant J, Raap A, Hagemeijer A, et al. (1992) Can, a putative oncogene associated with myeloid leukemogenesis, may be activated by fusion of its 3' half to different genes: characterization of the set gene. Mol Cell Biol 12: 3346-55. » CrossRef » PubMed » Google Scholar

50. Wilm M, Shevchenko A, Houthaeve T, Breit S, Schweigerer L, et al. (1996) Femtomole sequencing of proteins from polyacrylamide gels by nano-electrospray mass spectrometry. Nature 379: 466-9. » CrossRef » PubMed » Google Scholar

The Lyn kinase C-lobe mediates Golgi export of Lyn through conformation-dependent ACSL3 association

Yuuki Obata[1], Yasunori Fukumoto[1], Yuji Nakayama[1], Takahisa Kuga[1], Naoshi Dohmae[2] and Naoto Yamaguchi[1,*]

[1]Department of Molecular Cell Biology, Graduate School of Pharmaceutical Sciences, Chiba University, Chiba 260-8675, Japan
[2]Biomolecular Characterization Team, RIKEN, 2-1 Hirosawa, Wako, Saitama 351-0198, Japan
*Author for correspondence (nyama@p.chiba-u.ac.jp)

Summary

The Src-family tyrosine kinase Lyn has a role in signal transduction at the cytoplasmic face of the plasma membrane upon extracellular ligand stimulation. After synthesis in the cytoplasm, Lyn accumulates on the Golgi and is subsequently transported to the plasma membrane. However, the mechanism of Lyn trafficking remains elusive. We show here that the C-lobe of the Lyn kinase domain is associated with long-chain acyl-CoA synthetase 3 (ACSL3) on the Golgi in a manner that is dependent on Lyn conformation but is independent of its kinase activity. Formation of a closed conformation by CSK prevents Lyn from associating with ACSL3, resulting in blockade of Lyn export from the Golgi. Overexpression and knockdown of ACSL3 accelerates and blocks Golgi export of Lyn, respectively. The post-Golgi route of Lyn, triggered by ACSL3, is distinct from that of vesicular stomatitis virus glycoprotein (VSV-G) and of caveolin. Moreover, an ACSL3 mutant lacking the LR2 domain, which is required for the catalytic activity, retains the ability to associate with Lyn and accelerate Golgi export of Lyn. These results suggest that initiation of Golgi export of Lyn involves association of ACSL3 with the Lyn C-lobe, which is exposed to the molecular surface in an open conformation.

Key words: Src-family tyrosine kinases, Trafficking, Lyn, Kinase domain, Golgi, ACSL3

Introduction

Src-family tyrosine kinases, which are non-receptor-type tyrosine kinases, consist of proto-oncogene products and structurally related proteins and include at least eight highly homologous proteins: Src, Lyn, Yes, Fyn, Fgr, Hck, Lck and Blk (Brown and Cooper, 1996; Thomas and Brugge, 1997). Src-family tyrosine kinases have crucial roles in the regulation of cell proliferation, differentiation, migration and cell-shape changes (Thomas and Brugge, 1997). Src, Lyn, Yes and Fyn are widely expressed in a variety of cell types, whereas Blk, Hck, Fgr and Lck are found primarily in hematopoietic cells (Bolen and Brugge, 1997; Thomas and Brugge, 1997).

Src-family tyrosine kinases are composed of: (1) an N-terminal Src homology (SH) 4 domain, (2) a poorly conserved 'unique' domain, (3) an SH3 domain, which can bind to specific proline-rich sequences, (4) an SH2 domain, which can bind to specific sites of tyrosine phosphorylation, (5) an SH1 tyrosine kinase catalytic domain and (6) a C-terminal negative regulatory tail for autoinhibition of the kinase activity (Brown and Cooper, 1996). The tyrosine kinase activity of Src-family kinases is repressed through CSK-induced 'closed conformation' as a result of the intramolecular binding of the SH2 domain to the tyrosine-phosphorylated tail catalyzed by CSK-family kinases and the SH3 domain to the SH2-kinase linker (Brown and Cooper, 1996; Sicheri et al., 1997; Xu et al., 1997). Src-family tyrosine kinases can interact with a large number of upstream regulators and downstream substrates via SH2- and SH3-domain-mediated protein-protein interactions (Pawson, 1995; Thomas and Brugge, 1997; Blume-Jensen and Hunter, 2001).

Src-family tyrosine kinases, which are classified as cytosolic enzymes, localize at the cytoplasmic face of the plasma membrane

through post-translational lipid modification (Resh, 1994), but an appreciable fraction is found at intracellular compartments, such as late endosomes, lysosomes, the Golgi, secretory granules and the nucleus (Kaplan et al., 1992; Ley et al., 1994; Möhn et al., 1995; Bijlmakers et al., 1997; Yamaguchi et al., 2001; Kasahara et al., 2004; Kasahara et al., 2007a; Chu et al., 2007; Grimmler et al., 2007; Ikeda et al., 2008; Sato et al., 2009; Takahashi et al., 2009). Distinctive localizations of individual members of Src-family kinases have been implicated in their specific functions.

Lyn, a member of Src-family tyrosine kinases, is widely expressed in a variety of organs, tissues and cell types, including epithelial, hematopoietic and neuronal cells, and has an important role in signal transduction at the cytoplasmic face of the plasma membrane (Tsukita et al., 1991; Hibbs et al., 1995; Nishizumi et al., 1995; Hirao et al., 1998; Hayashi et al., 1999; Sheets et al., 1999; Tada et al., 1999; Rivera and Olivera, 2007; Kuga et al., 2007; Kuga et al., 2008; Sohn et al., 2008). We recently showed that newly synthesized Lyn in the cytoplasm accumulates on Golgi membranes and is subsequently transported to the plasma membrane along the secretory pathway in a manner that is dependent on the Lyn kinase domain (Kasahara et al., 2004; Sato et al., 2009). The Lyn kinase domain is also required for targeting of Lyn to caveolin-positive Golgi membranes (Ikeda et al., 2009), which suggests that this domain has a crucial role in Lyn trafficking in addition to its role in catalysis of substrate tyrosine phosphorylation. We further showed that Lyn tyrosine-phosphorylates annexin II on Golgi membranes, leading to the translocation of annexin II from the Golgi complex to the endoplasmic reticulum (ER) (Matsuda et al., 2006), suggesting that Lyn functions not only at the plasma membrane but also at the Golgi complex. Although the localization of Lyn is crucial for its
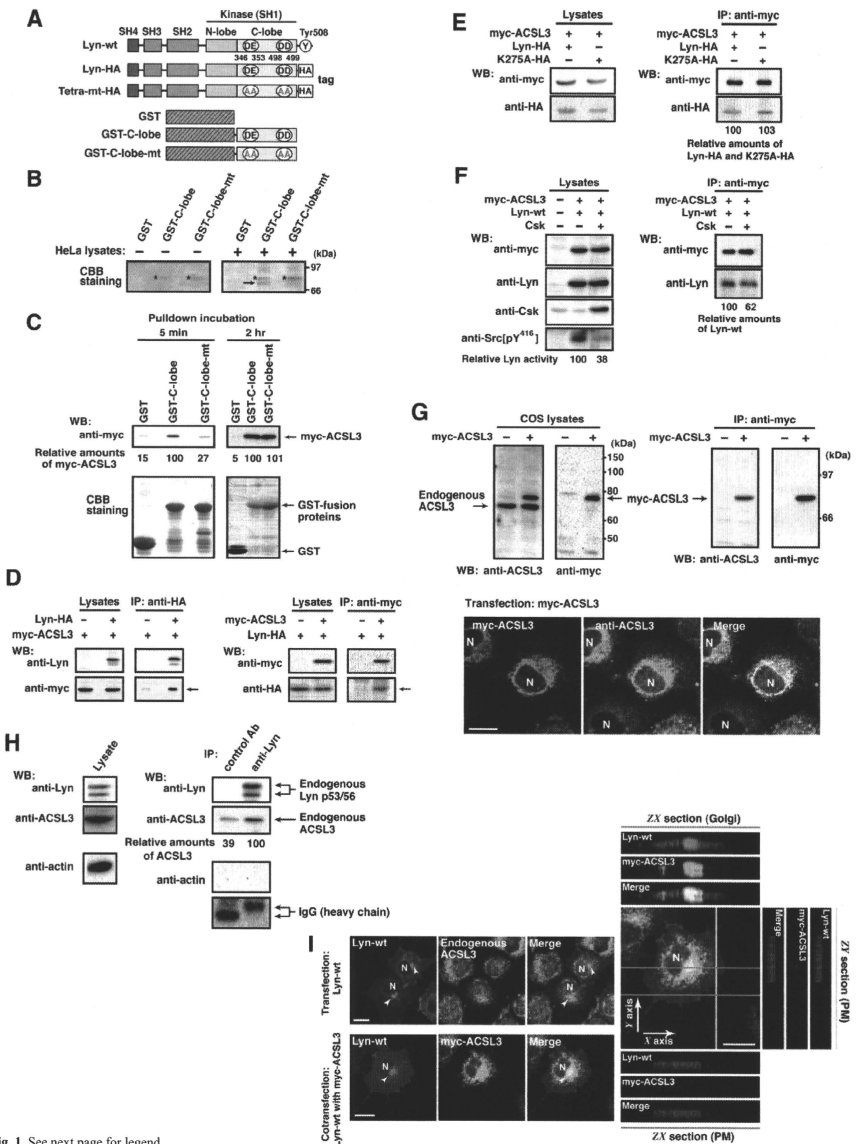
Fig. 1. See next page for legend.

Fig. 1. Association of Lyn with ACSL3. (A) Schematic representations of Lyn constructs, including wild-type Lyn (Lyn-wt). The Src homology (SH) domains, the N- and C-terminal lobes (N- and C-lobes) of the kinase domain, the alanine mutations of Asp346, Glu353, Asp498 and Asp499 (A in red) in the C-lobe, the negative-regulatory tyrosine residue (Y), and the HA and GST tags are indicated. (B) Triton X-100 lysates prepared from HeLa cells were used for pulldown experiments with GST, GST-C-lobe or GST-C-lobe-mt, and proteins pulled down after incubation for 2 hours at 4°C were stained with Coomassie brilliant blue (CBB). An arrow indicates a protein at 70 kDa that preferentially associated with the C-lobe (wild-type). Asterisks indicate a protein derived from *E. coli*. Molecular size markers in kDa are indicated on the right. (C) COS-1 cells were transfected with Myc-ACSL3 and cultured for 24 hours. Triton X-100 lysates were used for pulldown experiments with GST, GST-C-lobe or GST-C-lobe-mt, and amounts of Myc-ACSL3 pulled down after incubation for 5 minutes or 2 hours at 4°C were assayed by immunoblotting with anti-Myc antibody. Amounts of Myc-ACSL3 are expressed as values relative to those pulled down with GST-C-lobe. GST proteins were visualized by CBB staining. (D) COS-1 cells transfected with Lyn-HA, Myc-ACSL3 or Lyn-HA plus Myc-ACSL3 were cultured for 13 hours (left) or 24 hours (right). Myc-ACSL3 and Lyn-HA were immunoprecipitated from Triton X-100 cell lysates with anti-Myc (left) and anti-HA (right) antibody, respectively. Immunoblotting was performed for Myc and HA (left) or Lyn and Myc (right). Arrows indicate coimmunoprecipitated bands. (E) COS-1 cells were cotransfected with Lyn-HA plus Myc-ACSL3 or Lyn(K275A)-HA plus Myc-ACSL3 and cultured for 24 hours. Myc-ACSL3 was immunoprecipitated from Triton X-100 cell lysates with anti-Myc antibody. Immunoblotting was performed for Myc and HA. The amount of Lyn(K275A)-HA in the Myc-ACSL3 immunoprecipitate is expressed as the value relative to that of Lyn-HA in the Myc-ACSL3 immunoprecipitate after normalization with Myc-ACSL3 protein levels. (F) COS-1 cells transfected with or without CSK were cultured for 8 hours, and then cotransfected with Lyn-wt plus Myc-ACSL3. After subsequent culture, Myc-ACSL3 was immunoprecipitated from Triton X-100 cell lysates with anti-Myc antibody. Immunoblotting was performed for Myc, Lyn, CSK and phosphorylated Src (pY^{416}). Lyn activities were normalized to the amounts of Lyn present in the lysates, and amounts of coimmunoprecipitated Lyn were normalized to those of Myc-ACSL3 present in the immunoprecipitates. (G) (Upper panels) COS-1 cells were untransfected or transfected with Myc-ACSL3 and cultured for 24 hours. Myc-ACSL3 was immunoprecipitated from Triton X-100 cell lysates with anti-Myc antibody. Cell lysates (left) and immunoprecipitates (right) were immunoblotted with anti-ACSL3 and anti-Myc antibodies. Molecular size markers in kDa are indicated on the right. Lower panels show COS-1 cells transfected with Myc-ACSL3 and cultured for 24 hours. Cells were doubly stained with anti-Myc (red) and anti-ACSL3 (green) antibodies. Colocalizations of Myc-ACSL3 with endogenous ACSL3 expression are seen in the image. N, nucleus. Scale bar: 20 μm. (H) Endogenous Lyn was immunoprecipitated from Triton X-100 HeLa cell lysates with anti-Lyn antibody. MOPC21 was used as a control antibody. Immunoblotting was performed for Lyn, ACSL3 and actin. Amounts of endogenous ACSL3 are expressed as relative values. Endogenous Lyn p53 and Lyn p56 are two alternative spliced isoforms of Lyn. (I) (Top panels) COS-1 cells transfected with Lyn-wt cultured for 18 hours doubly stained with anti-Lyn (red) and anti-ACSL3 (green) antibodies. (Middle panels) COS-1 cells cotransfected with Lyn-wt plus Myc-ACSL3 cultured for 12 hours and doubly stained with anti-Lyn (red) and anti-Myc (green) antibodies. Arrowheads indicate the perinuclear region. (Bottom panels) Orthogonal sections viewing axial directions (*ZX* and *ZY*) at the lines in red, blue, and yellow are shown surrounding main image. N, nucleus. Scale bars: 20 μm.

functions, the mechanism of the intracellular trafficking of Lyn remains elusive.

In this study, we investigate the mechanism of the trafficking of Lyn from the Golgi to the plasma membrane. We show that the C-lobe of the Lyn kinase domain associates with ACSL3 when Lyn has an open conformation, thereby initiating the export of Lyn from the Golgi. Our results provide the first demonstration of a direct role of the Lyn kinase C-lobe in Golgi export of Lyn.

Results
Association of the Lyn kinase C-lobe with ACSL3
We previously showed that the trafficking of newly synthesized Lyn from the Golgi to the plasma membrane involves the four charged amino acid residues (Asp346, Glu353, Asp498 and Asp499) in the C-lobe of the Lyn kinase domain (Kasahara et al., 2004). We thus hypothesized that the Lyn C-lobe has a role in trafficking through a protein-protein interaction. To search for a protein that associates with the Lyn C-lobe, we constructed a glutathione-S-transferase (GST)-Lyn C-lobe fusion protein (GST-C-lobe), which encompasses amino acids 326-506 in Lyn (Fig. 1A). We found that a 70 kDa protein (p70) was pulled down with GST-C-lobe but not with GST alone from Triton-X-100-treated HeLa cell lysates (Fig. 1B). We then constructed GST-C-lobe-mt, an alanine-substitution mutant (Fig. 1A). p70 could be pulled down with GST-C-lobe-mt but to a lesser extent than seen with GST-C-lobe (Fig. 1B), suggesting that p70 preferentially associates with the intact C-lobe. Consequently, the p70 band was excised and subjected to proteolytic cleavage followed by MALDI-TOF-MS. The peptide derived from p70 (VLSEAAISASLEK) exhibited 100% identity with the amino acid sequence of human long-chain acyl-CoA synthetase-3 (ACSL3; EC 6.2.1.3).

To verify the association of the Lyn C-lobe with ACSL3 in vitro, we expressed N-terminally Myc-tagged ACSL3 (Myc-ACSL3; Fig. 4A) in COS-1 cells. Upon 5-minute incubation with Myc-ACSL3-containing Triton X-100 cell lysates at 4°C Myc-ACSL3

was pulled down preferentially with GST-C-lobe rather than GST-C-lobe-mt, although upon incubation at 4°C for 2 hours, Myc-ACSL3 could be pulled down with GST-C-lobe-mt to a similar extent as that with GST-C-lobe (Fig. 1C). Next, we tested whether Lyn was associated with ACSL3 in vivo. When Lyn-HA and Myc-ACSL3 were coexpressed in COS-1 cells, Lyn-HA was coimmunoprecipitated with Myc-ACSL3 and vice versa (Fig. 1D). Similarly to Lyn-HA, kinase-inactive Lyn(K275A)-HA was coimmunoprecipitated with Myc-ACSL3 (Fig. 1E). These results suggest that Lyn is associated with ACSL3 in a manner that is independent of the Lyn kinase activity.

We hypothesized that the charged residues in the C-lobe are exposed to the molecular surface of Lyn when it is in an open conformation (Kasahara et al., 2004). Since a closed, repressed conformation of Src-family kinases is created by CSK-mediated phosphorylation of their C-terminal tyrosine residue, we examined whether overexpression of CSK could inhibit the association of Lyn with ACSL3. COS-1 cells were triply cotransfected with wild-type Lyn (Lyn-wt), Myc-ACSL3 and CSK. Western blot analysis confirmed that the kinase activity of Lyn-wt was decreased because of the induction of a closed conformation of Lyn-wt by overexpression of CSK. Intriguingly, the association of Lyn-wt with Myc-ACSL3 was affected by CSK overexpression (Fig. 1F), suggesting that a closed conformation of Lyn inhibits its association with ACSL3.

Using anti-ACSL3 antibody that recognises both Myc-ACSL3 and endogenous ACSL3 in COS-1 and HeLa cells (Fig. 1G; supplementary material Fig. S1), we showed that two alternative spliced isoforms of endogenous Lyn were associated with endogenous ACSL3 (Fig. 1H). Although a fraction of ACSL3 appeared in the immunoprecipitate with control antibody, actin did not appear in the immunoprecipitates, suggesting that ACSL3 might nonspecifically interact with immunoglobulin and/or protein-G-bound beads. Furthermore, ACSL3 was seen with the Golgi caveolin and β-1,4-galactosyltransferase (GalT) where Lyn